Characterization of polymeric membranes for non-aqueous separations

Characterization of polymeric membranes for non-aqueous separations

PROEFSCHRIFT

ter verkrijging van de graad van doctor aan de
Technische Universiteit Eindhoven, op gezag van de
Rector Magnificus, prof.dr.ir. C.J. van Duijn, voor een
commissie aangewezen door het College voor
Promoties in het openbaar te verdedigen
op donderdag 6 december 2007 om 16.00 uur

door

Ana Maria Manito Pereira

geboren te Abrantes, Portugal

Dit proefschrift is goedgekeurd door de promotor:

prof.dr.ir. J.T.F. Keurentjes

The content of this thesis had the financial support of the Marie Curie Industrial host fellowship program (contract HPMI-CT-2002-00181)

A catalogue record is available from the Library Eindhoven University of Technology

ISBN: 978-90-386-1148-8

Learning is experiencing the world

Contents

Summary

Characterization of polymeric membranes for non-aqueous separations

The industrial application of solvent resistant nanofiltration (SRNF) membranes for solvent purification has grown considerably in the last decade. The number of solvent/membrane systems is increasing and consequently, the need for characterization of chemical and physical phenomena, i.e. sorption, swelling, compaction and mobility. This thesis provides a tool box with characterization methods that are aimed to be independent of the solvent and membrane material and to provide results focused on the transport determining layer of the membrane.

In Chapter 2 the determining transport mechanism of three similar solvents (methanol, ethanol and 1-butanol) in a silicon-type SRNF membrane has been studied. The results suggest that diffusion alone can not explain the transport of alcohols and an additional transport mechanism takes place. Assuming the additional mechanism to be viscous in nature allows a fit of a flux expression to the experimental data using one single fitting parameter. For 1-butanol, the contribution of the additional mechanism is only small. In contrast, for the smaller methanol and ethanol the contribution of viscous flow is very high. This is in contrast with observations in literature for similar systems, signifying a limited applicability of state-of-the-art models for predicting solvent transport through SRNF membranes.

Chapter 3 presents a generic method that allows the determination of retention behavior in non-aqueous solvent filtration. The method has limited restrictions with respect to solute solubility and is independent of the solvent studied. Using a low concentration of polyethylene glycol 1000 with a broad molecular weight distribution, combined with a powerful analytical technique such

as mass spectroscopy, a single retention experiment produces a full retention curve. In this way, the molecular weight cut-off (MWCO) of a membrane can be directly determined and the cost and time of the experimental procedure is reduced. Retention has been shown to be mostly dependent on the rate and mechanism of solvent transport. For transport that is solely or partially viscous, dragging effects cause the retention of small PEG oligomers to be low. For transport determined by diffusion, dragging effects are insignificant and retention is high (98%) irrespective of the size and shape of the solute molecule.

Chapters 4 and 6 show the versatility of attenuated total reflectance spectroscopy infrared (ATR-IR) to determine in-situ sorption and compaction in the active layer of a cellulose acetate (CA) membrane and a silicon-type SRNF membrane, respectively. Preferential sorption of water has been measured in a CA membrane for water/methanol and water/ethanol mixtures. The results are in accordance with literature. The extent of compaction of the transport determining layer of the commercial SRNF membrane has been determined under different pressure conditions. Results show that reduction in thickness of the entire membrane can not be directly related to the reduction in density of the active layer. Comparison with permeation experiments under the same conditions show the importance of measuring both swelling and compaction simultaneously.

Chapter 5 shows the development of two straightforward techniques to measure swelling: mechanically using a micrometer and optically using an interferometer. Both methods allow the study of the dynamic swelling behavior and yield similar results. Different polymer layers present in the membrane show different contributions to swelling. Comparison of the dynamics of swelling and sorption reveals that these two phenomena, although interdependent, do not start simultaneously and are not comparable in magnitude. For this reason, if the extent of sorption is interpreted as a direct measure for the extent of swelling, incorrect conclusions can be drawn.

Chapter 7 concludes the thesis by taking a look at the impact of the work developed. Furthermore, the future possibilities for developments regarding the characterization, prediction and process monitoring are discussed.

Chapter 1

Introduction

1.1 Nanofiltration

Nanofiltration is a pressure driven filtration process that has been introduced initially for water purification. In nanofiltration, the separation is based on both the size and the charge of the permeating components. The process is characterized by a low molecular weight cut-off (MWCO) (approximately 100 to 1000 Dalton) and a high retention for multivalent ions as compared to monovalent ions [1]. Applications include the food, metal and clothing industry, for which a good overview can be found in literature [2]. Initially nanofiltration membranes were considered “something in between reverse osmosis (RO) and ultrafiltration (UF)”. Compared to RO membranes, rejection values are much lower and monovalent ions are retained only to a minor extent. Compared to UF, the retention is much higher and the flux is much lower.

Common materials for nanofiltration membranes include cellulose acetate, polyamide and polysulfone. Membranes are mostly prepared by phase inversion but other techniques include interfacial polymerization and polymer coating. The parameters determining permeation performance of aqueous nanofiltration systems have been widely discussed in literature [3-7] and models are available for the prediction of transport in these systems where water is the main solvent.

1.2 Solvent resistant nanofiltration

Organic solvents are widely used in industry and in many cases have to be discarded after use. For solvent recovery many conventional and energy intensive processes are used, such as distillation, evaporation and extraction [8,9]. Compared to these separation techniques, solvent

recovery using membrane filtration can have advantages; a reduced number of separation steps to achieve a high degree of purity, combined with a low energy requirement. In addition, compared to traditional separation techniques, membrane technology allows solvent recovery with a low loss of product. A sharp increase of solvent filtration occurred during the late 90's, when the potential to reduce energy costs and to comply with environmental regulations was first recognized. In 1998, the first plant scale solvent nanofiltration process started at Exxon Mobil in the United States. In this process (Max Dewax^{TM}), solvent with an oil content bellow 1% is recovered from a lubricant de-waxing unit [10].

Figure 1.1 illustrates the number of publications during the last 16 years making a distinction between water treatment (aqueous nanofiltration) and solvent resistant nanofiltration (non-aqueous nanofiltration). The annual publication of patents related to solvent nanofiltration has been relatively constant, approximately 1 to 2 per year for the last 10 years. Figure 1.2 shows the relative contribution of different types of publications related to the field of solvent nanofiltration.

The low number of publications for non-aqueous nanofiltration reveals the infancy of this technology. The increase in the number of publications indicates an increase in interest in the subject from the scientific community. The development has been induced by a need to understand and better predict nanofiltration processes for solvent applications. Also, with the development of new applications [1] new questions and research areas are being created.

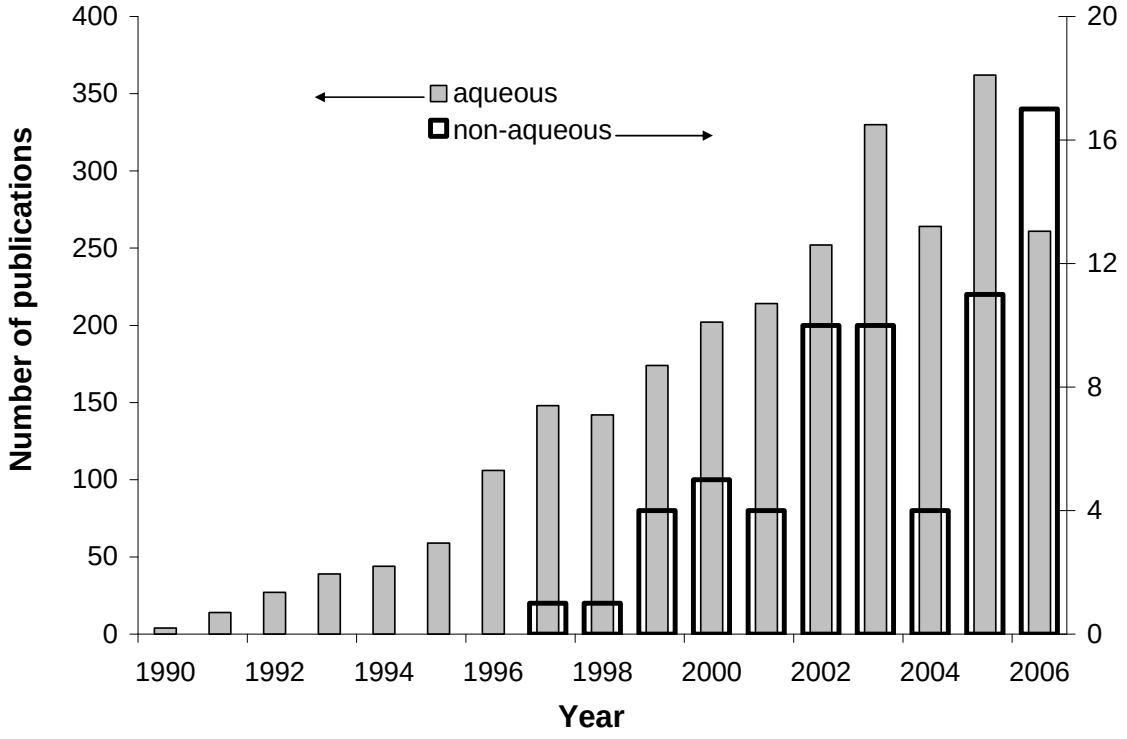

Figure 1.1: Number of publications per year related to nanofiltration for aqueous and non-aqueous solvent applications [11].

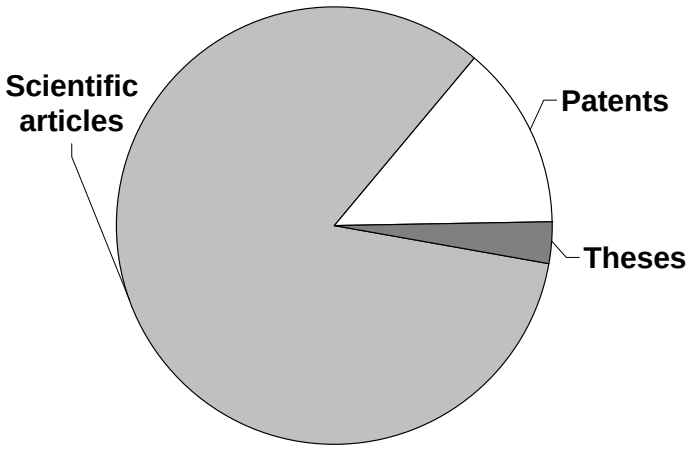

Figure 1.2: Relative numbers of different types of publications related to the field of solvent nanofiltration [11].

1.3 Membranes and materials

The opportunities and restrictions initially encountered of using existing aqueous nanofiltration membranes for solvent applications have been discussed in literature by Ebert and Cuperus [12]. The initial limitations were related to poor chemical resistance and performance, and the high price in the case of ceramic membranes [1]. In order to improve chemical resistance and separation performance new membrane materials have been developed in the last 15 years. Several polymer materials have been used; the most common include polyamides (PA), polyimides (PI) and polydimethylsiloxane (PDMS). To reduce swelling and compaction effects and to increase chemical resistance, these materials are highly crosslinked and have different properties as compared to the original polymers present in aqueous nanofiltration membranes.

In the case of aqueous nanofiltration, the main solvent, i.e. water, is common to all applications. Therefore, the extent of compaction, swelling and sorption of a membrane can be extrapolated to all applications. In contrast, non-aqueous nanofiltration membrane polymers will respond differently to different solvents, requiring measurements to be made for all systems.

1.4 Problem definition

From a very early stage literature has shown an emphasis on finding a general model for the prediction of separation performance in non-aqueous nanofiltration systems [13-19], starting from existing theory developed for aqueous nanofiltration. In addition to the fact that solvent/membrane interactions are different from system to system, the theoretical description of solvent nanofiltration is complicated by the effects of swelling and compaction. The extent of these phenomena depends on the applied process conditions, such as temperature and pressure. Structural changes due to swelling and compaction will strongly affect the pore size and openness of the selective layer, and will consequently influence separation performance.

The problem is schematically represented in Figure 1.3 where each piece of the puzzle represents a parameter that will have an important influence on the nanofiltration process. Although the puzzle depicted in Figure 1.3 is not complete, it contains some of the major issues to be addressed for understanding non-aqueous nanofiltration. Moreover, the pieces of the puzzle are

interrelated, e.g. sorption and mobility are strongly correlated with swelling and compaction. The relations between the pieces of the puzzle will be different for each solvent/membrane system.

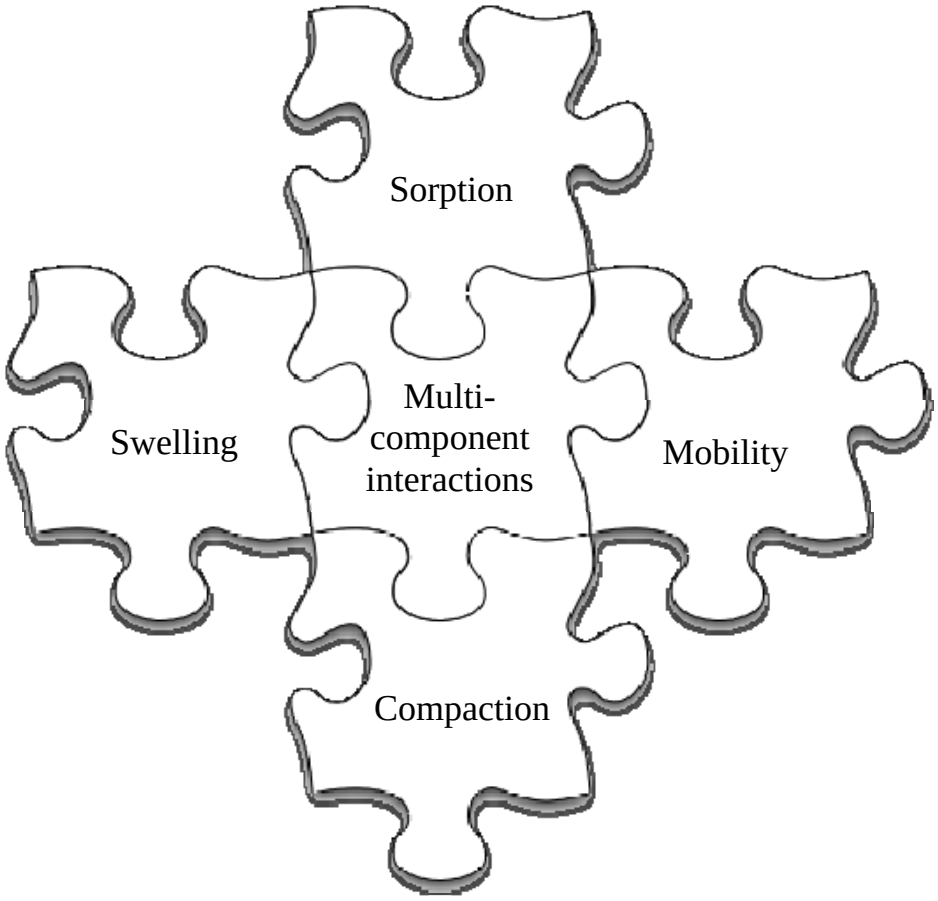

Figure 1.3: Schematic representation of the phenomena influencing the performance of a polymeric membrane in different solvent environments.

In this thesis an attempt will be made to provide tools that can be used for measurement of the relevant phenomena in a feasible timescale for commercial asymmetric membranes. The performance of these membranes is determined by a very thin active layer, typically 1 to 2 μm thick. This layer is an integral part of the membrane and separating it from the support structure while keeping the polymer properties unchanged is in general not possible. In addition, lab scale preparation of representative samples is hindered by protection of intellectual properties of

membrane manufacturers. At this moment it is not possible to adequately measure in-situ the relevant parameters of a thin layer using available characterization techniques. Most methods require a stand alone sample of the polymer, difficult experimental set-ups and at times complex theoretical background.

1.5 Aim of the thesis

The objective of this work is to provide a tool box with methods that can be used to acquire knowledge needed for relevant solvent/membrane/solute systems. Preferably, the methods should be independent of the solvent and membrane; they should allow characterization of any polymeric membrane in any solvent environment. Moreover, each tool should comply with making measurements easy, fast and understandable.

1.6 Scope of the thesis

In **Chapter 2** the determining mechanism of transport of 3 solvents of similar chemistry (methanol, ethanol and 1-butanol) is studied. In **Chapter 3** a method is presented to determine the retention as a function of molecular weight for a commercial membrane, using one single experiment. The method is independent of the solvent/membrane/solute system. In **Chapter 4** attenuated total reflectance infrared (ATR-IR) is used to determine in-situ solvent competitive sorption in the active layer of a polymeric membrane. In **Chapter 5** two undemanding methods are presented to measure swelling, i.e. the change in thickness, of commercial nanofiltration membranes in different solvents. In **Chapter 6** ATR-IR is used to measure compaction of nanofiltration membranes in different solvents. Finally in **Chapter 7** the implications of the developed tool box and perspectives for future research are discussed.

References

[1] A. I. Shäfer, A. G. Fane, T. D. Waite, Nanofiltration principles and applications, Elsevier, Oxford, Chapter 1, (2005)

[2] J. M. K Timmer, Properties of nanofiltration membranes; model development and industrial applications, PhD thesis, Technische Universiteit Eindhoven (2001) ISBN 90-386-2872-2

[3] B. van der Bruggen, L. Braeken, C. Vandecasteele, Evolution of parameters describing flux decline in nanofiltration of aqueous solutions containing organic compounds, Desalination 147 (2002) 281-288

[4] W. R. Bowen, J. S. Welfoot, Modeling of membrane nanofiltration – pore size distribution effects, Chem. Eng. Sci. 57 (2002) 1393-1407

[5] E. M. Tsui, M. Cheryan, Characteristics of nanofiltration membranes in aqueous ethanol, J. Memb. Sci. 237 (2004) 61-69

[6] G. Bargeman, J. M. Vollenbroek, J. Straatsma, C. G. P. H. Schröen, R. M. Boom, Nanofiltration of multicomponent feeds. Interactions between neutral and charged components and their effect on retention, J. Memb. Sci. 247 (2005) 11-20

[7] K. Boussu, Y. Zhang, J. Cocquyt, P. van der Meeren, A. Volodin, C. van Haesendonck, J. A. Martens, B. van der Bruggen, Characterization of polymeric nanofiltration membranes for systematic analysis of membrane performance, J. Memb. Sci. 278 (2006) 418-427

[8] S. S. Köseoglu, D. E. Engelgau, Membrane applications and research in the edible oil industry: an assessment, J. Am. Oil Chem. Soc. 67 (1990) 239-249

[9] S. S. Köseoglu, J. T. Lawhon, E. W. Lusas, Membrane processing of crude vegetable oil: pilot plant scale removal of solvent from oil miscellas, J. Am. Oil Chem. Soc. 67 (1990) 315-322

[10] http://www.**exxonmobil**.com/Refiningtechnologies/lubes/mn_**max_dewax**.html (2007)

[11] Scifinder Scholar 2006, Chemical abstracts data base, Am. Chem. Soc. March 2007

[12] K. Ebert, F. P. Cuperus, Solvent resistant nanofiltration membranes in edible oil processing, J. Memb. Tech. 107 (1999) 5-8

[13] W. R. Bowen, H. Mukhtar, Characterization and prediction of separation performance of nanofiltration membranes, J. Memb. Sci. 112 (1996) 263-274

[14] J. A. Whu, B. C. Baltzis, K. K. Sirkar, Modeling of nanofiltration – assisted organic synthesis, J. Memb. Sci. 163 (1999) 319-331

[15] D. R. Machado, D. Hasson, R. Semiat, Effect of solvent properties on permeate flow through nanofiltration membranes. Part I: investigation of parameters affecting solvent flux, J. Memb. Sci. 163 (1999) 93-102

[16] U. Cocchini, C. Nicolella, A. Livingston, Countercurrent transport of organic and water molecules through thin film composite membranes in aqueous-aqueous extractive membrane processas. Part II: theoretical analysis, Chem. Eng. Sci. 57 (2002) 4461-4473

[17] J. A. Whu, B. C. Baltzis, K. K. Sirkar, Nanofiltration studies of larger organic microsolutes in methanol solutions, J. Memb. Sci. 170 (2000) 159-172

[18] S. Chen, D. Chang, R. Liou, C. Hsu, S. Lin, Preparation and separation properties of polyamide nanofiltration membranes, J. Appl. Polym. Sci. 83 (2002) 1112-1118

[19] X. J. Yang, A. G. Livingston, L. F. dos Santos, Experimental observations of nanofiltration with organic solvents, J. Memb. Sci. 190 (2001) 45-55

Chapter 2

Transport of alcohols through solvent resistant nanofiltration membranes: A molecular size dependent contribution of diffusion and viscous transport

---

The fluxes of methanol, ethanol and 1-butanol through a commercial silicon type membrane (Solsep 030206) have been measured as a function of transmembrane pressure and temperature. All three alcohols show a linear dependence of the flux on transmembrane pressure difference and no hysteresis effects have been observed. The results are explained by considering transport to occur via a combination of diffusion and viscous transport. The relative contribution of viscous transport is highly dependent on the molecular size of the alcohol. Even for the three almost similar solvents a different mechanism prevails. In the case of the relatively bulky 1-butanol diffusion is predominant and a low flux is observed. On the other hand, for the smaller methanol and ethanol the viscous contribution predominates.

2.1 Introduction

2.1.1 Aqueous nanofiltration

Nanofiltration membranes for aqueous systems have been commercially available since the 1970s. Materials and applications for these membranes include cellulose acetate for water treatment, polyelectrolyte complexes for concentration and demineralization of proteins and organic solutes, and polyamide used in seawater desalination [1]. Mass transport in such applications has been studied extensively and recently Bowen et al. [2] has published a thorough analysis of existing models for aqueous systems.

2.1.2 Non-aqueous nanofiltration

Organic solvents are extensively used in the pharmaceutical, (petro)chemical and food industry. Solvent recovery processes, such as nanofiltration, are becoming increasingly important. Polymeric solvent resistant nanofiltration (SRNF) membranes generally possess a highly crosslinked top layer. Common materials for the top layer include polydimethylsiloxane (PDMS), polyamide (PA) and polyimide (PI) [1]. The existing theory for aqueous nanofiltration cannot be used for SRNF membranes in a straightforward manner. Various models have been proposed in literature relating solvent transport to, for example, viscosity and solvent/polymer interactions [3-5] and several of these models have successfully been fitted to experimental data [6-12]. The major variable in all the studies is the solvent/membrane system. It has become apparent that applicability of currently available models is limited to particular solvent/membrane systems. A model that is successful for one specific system may fail for other systems. In this work we will show that for a commercial silicon type membrane even the small differences in size of methanol, ethanol and 1-butanol can lead to a shift from one predominant transport mechanism to another. For this, a flux equation including diffusion and convection has been fitted to experimental data at different pressures and temperatures.

2.2 Theory

We assume that transport of a small linear alcohol through a thin silicon type layer takes place by convective and diffusive transport, simultaneously. Correspondingly, the flux N of the solvent i through the membrane can be described by Equation 2.1, which can be obtained from for instance the Maxwell-Stefan approach [13]:

$$N_i = -c_i \left(\frac{\tilde{V}_i D_i}{RT} + \frac{A}{\eta_i} \right) \frac{\Delta p}{L} \qquad (2.1)$$

Here c is the concentration in the top layer, $\tilde{V}$ is the molar volume of the solvent, D the diffusion coefficient of the solvent in the membrane, R the universal gas constant, T the absolute temperature, η the viscosity of the solvent inside the polymer, p the pressure and L the thickness of the top layer. The parameter A is related to viscous transport and describes the proportionality between the flux and the pressure gradient, as in Darcy's law [14].

It should be noted that viscosity is a macroscopic property that should comply with the continuum hypothesis of matter [15]. For solvent molecules in a dense polymeric material this continuum hypothesis may fail as the solvent molecules in the polymer no longer form a continuum. As a result, in our case the concept of viscosity is debatable. The fundamental implications of this are beyond the scope of this study and we tacitly assume that the continuum approach can be applied.

Equation 2.1 contains the concentration and diffusion coefficient of the solvent in the polymer. For the three different alcohols in PDMS, experimental data are available for these variables [16, 17]. Within the temperature range applied in this study the solvent concentrations are assumed independent of temperature. Values of the diffusion coefficients at the different temperatures are extrapolated using the free volume theory (FVT) [18, 19] and normalized with respect to the experimental values at 40 °C (Table 2.1).

	0 °C	20 °C	40/50 °C *	Unit
Methanol	$0.89 \cdot 10^{-10}$	$1.5 \cdot 10^{-10}$	$2.5 \cdot 10^{-10}$	[m^2/s]
Ethanol	$0.6 \cdot 10^{-10}$	$1.1 \cdot 10^{-10}$	$2.3 \cdot 10^{-10}$	[m^2/s]
1-Butanol	$0.18 \cdot 10^{-10}$	$0.37 \cdot 10^{-10}$	$0.94 \cdot 10^{-10}$	[m^2/s]

Table 2.1: Diffusion coefficient values for methanol, ethanol and 1-butanol at 3 different temperatures (0, 20 and 40/50 °C) calculated using the FVT and experimental data at 40 °C [16]. * see section Experimental.

The term in Equation 2.1 that is related to viscous transport contains the viscosity of the solvent inside the polymer. The value of the viscosity is estimated using the FVT combined with the Stokes-Einstein relation [20], in a similar approach as presented by Kerkhof and Geboers [21]. The only independent parameter that remains undetermined is *A*. For each solvent the value of *A* can be adjusted to obtain a best fit of Equation 2.1 to experimental data.

2.3 Experimental

A commercial membrane (Solsep 030206, Solsep, the Netherlands) is used with an approximately 1 μm thick silicon type top layer. Methanol (99%), ethanol (99%) and 1-butanol (99%) were obtained from Sigma-Aldrich. Single component permeation was used in a batch membrane module (Figure 2.1) with a effective membrane area of 56.75 cm^2, maximum feed volume of 650 mL and a limiting pressure of 65 bar controlled by a relief valve. Experiments were carried out at 0, 20 and 50 °C, respectively. A temperature of 40 instead of 50 °C was used for methanol due to its low boiling point. For the temperature experiments, the module was heated/cooled using a water bath. Hysteresis experiments were performed by variation of the pressure from 40 to 10 bar (stepwise decrease of 10 bar), followed by a stepwise increase in pressure. At each pressure at least 10 flux values were acquired in a time frame of 50 minutes.

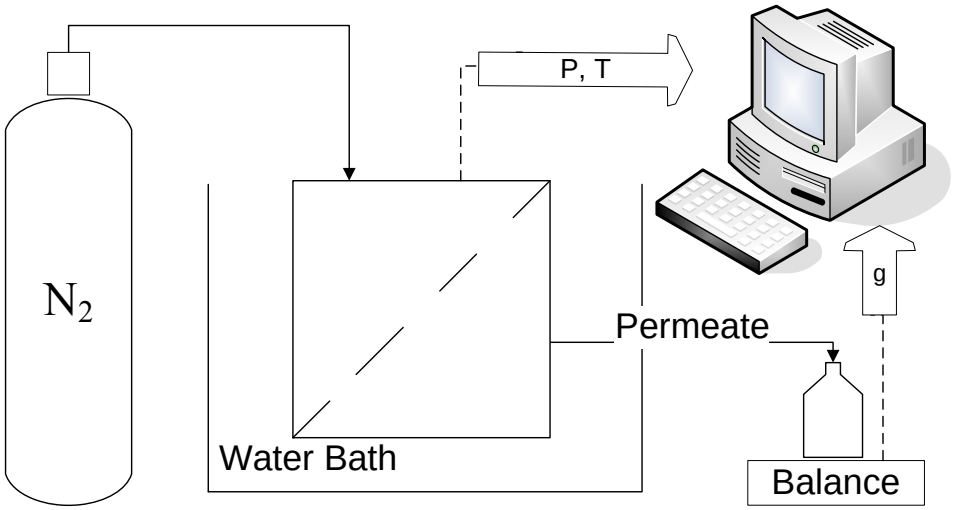

Figure 2.1: Schematic representation of the batch permeation set-up.

2.4 Results and discussion

In Figure 2.2 the evolution of the flux in time is presented for methanol. The transmembrane pressure has been varied to evaluate if hysteresis phenomena occur. No irreversible effects are evident from these results. The same behavior has been found for ethanol and 1-butanol. The results of the permeation experiments are summarized in Figure 2.3 a, b and c. In these graphs the flux is plotted as a function of the transmembrane pressure difference, at different temperatures. Each data point represents an average of 10 measured values; the error bars shown in Figure 2.3 b indicate the corresponding 95% confidence interval.

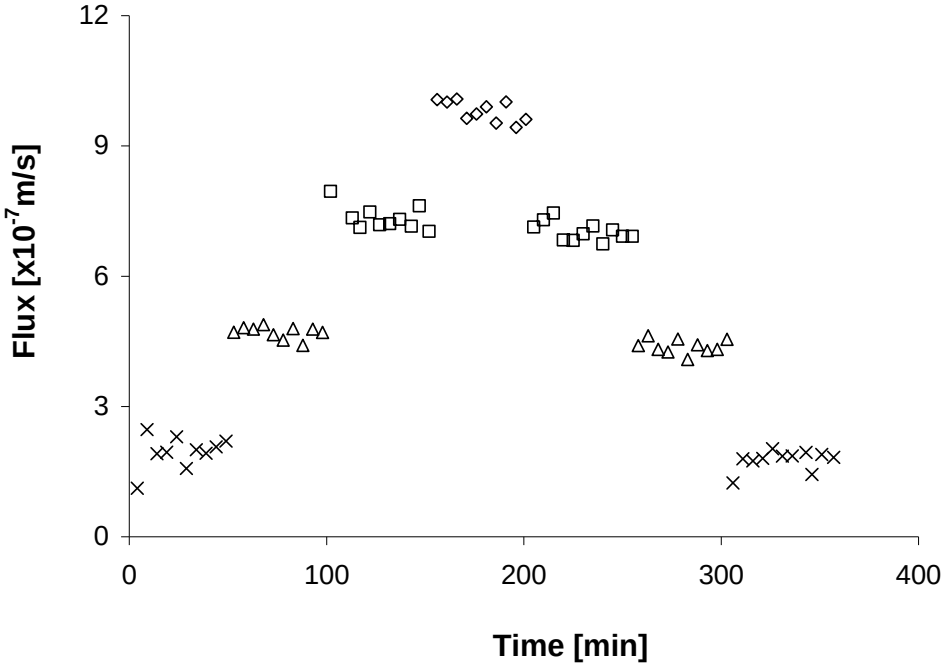

Figure 2.2: Flux of pure methanol through PDMS top layer solvent resistant nanofiltration membrane as a function of transmembrane pressure difference of: ◊ 40 bar; □ 30 bar; Δ 20 bar; x 10 bar.

a)

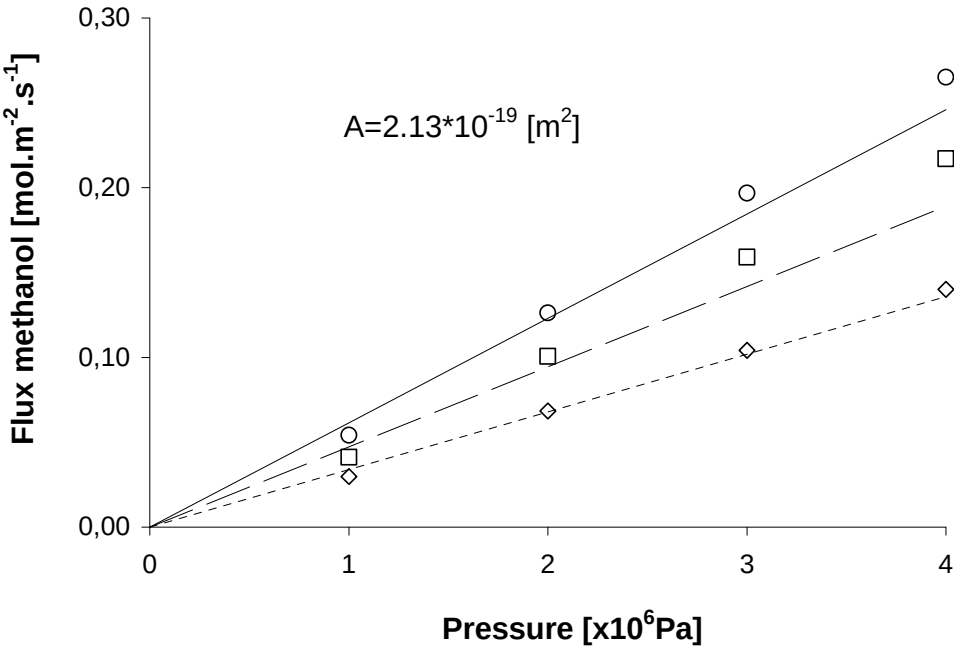

b)

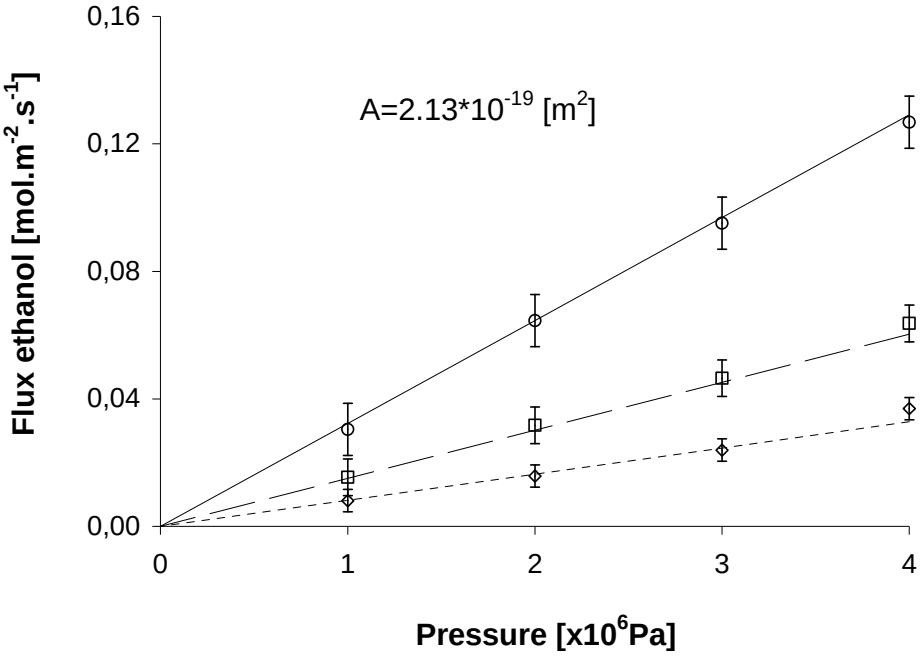

c)

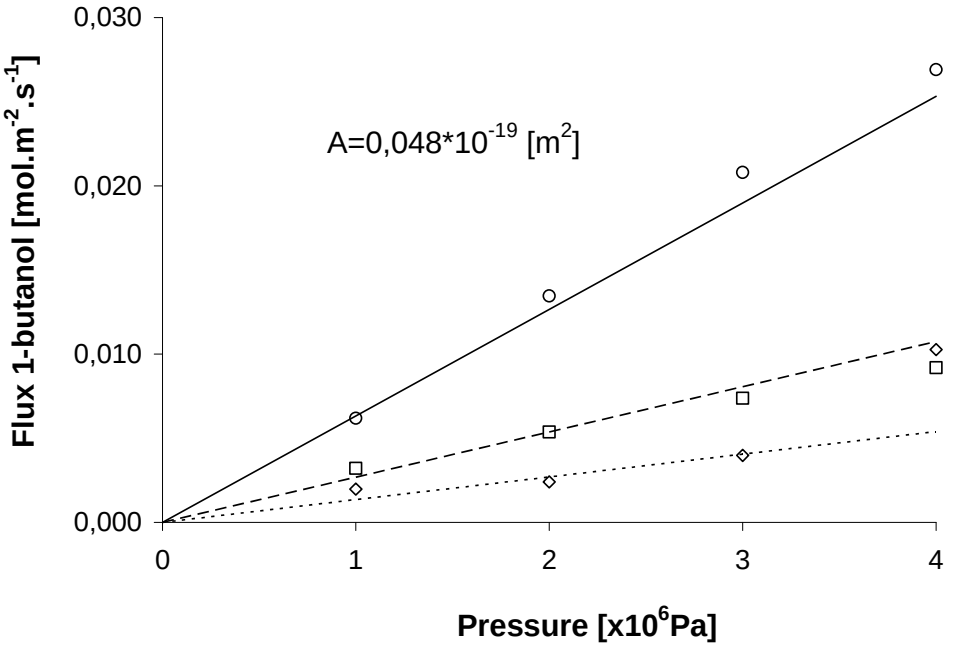

Figure 2.3: Flux as a function of transmembrane pressure difference at 3 different temperatures (◊ 0 °C; □ 20 °C; O 40/50 °C) for the case of a) methanol; b) ethanol and c) 1-butanol.

For all three alcohols the flux appears to be linearly proportional to the applied pressure difference and the parameter of proportionality shows an increase with temperature. The highest flux values are observed for methanol; at the same conditions the methanol flux is around two times larger as compared to the ethanol flux, and an order of magnitude higher as compared to the 1-butanol flux. Using the procedure described in the theory section, Equation 2.1 is fitted to the experimental data by allowing only the value of parameter *A* to be varied. The results are displayed as lines in Figure 2.3 and can be interpreted in terms of relative contributions of viscous transport and diffusive transport to the total flux (Table 2.1).

	Methanol	Ethanol	1-Butanol	Unit
A	$1.4 \cdot 10^{-19}$	$2.1 \cdot 10^{-19}$	$4.8 \cdot 10^{-21}$	[m^2]
Diffusive transport	0.5	8	76	[%]

Table 2.2: Diffusive transport contribution (%) to total flux of each of the 3 solvents used based on fitting parameter *A* (Equation 2.1) to experimental data shown in Figure 2.3.

The results indicate that the contribution of viscous transport is predominant in the flux of methanol and only 0.5% of the methanol flux originates from diffusion. For ethanol the contribution of diffusive transport is approximately 8%, indicating that 92% of the flux originates from viscous transport. In contrast, for 1-butanol the dominating transport mechanism is diffusion and only 24% of the flux originates from viscous transport. The differences between the different alcohols primarily originate from variation of the magnitude of the viscous flow contribution, rather than from variation in the magnitude of the contribution of diffusion.

For methanol the single parameter fit of Equation 2.1 to the experimental data is relatively inaccurate. Because for methanol the viscous contribution is predominant, the poor fit may be related to the unsophisticated estimation of the value for the viscosity. Moreover, as discussed in the theoretical section in our case the concept of viscosity is debatable.

For a different membrane obtained from the same supplier, Geens et al. [22] observed much higher flux values for various linear alcohols, as compared to our results. Their experimental data are successfully predicted by a pore flow model. Evidently, this approach would fail for the data presented in this study. This clearly illustrates the limited applicability of current models for predicting solvent transport in SRNF membranes.

2.5 Conclusions

The presented experimental data suggest that diffusion alone can not explain transport of alcohols through a silicon type solvent resistant nanofiltration membrane and an additional transport mechanism has to take place. For 1-butanol the contribution of the additional mechanism is only small. In contrast, for the smaller methanol and ethanol the contribution of viscous flow is very high. Assuming the additional mechanism to be viscous in nature allows a fit of the flux expression to the experimental data using only a single fitting parameter. Especially for the methanol the fit is poor, likely due to an inaccurate value for the viscosity. The results indicate that even for three almost similar solvents a different mechanism can dominate transport through a membrane. This is in contrast with the observations in literature for similar systems, signifying a limited applicability of state-of-the-art models for predicting solvent transport through SRNF membranes.

Acknowledgements

We would like to thank Joost Rooze and Vera Lourenço for all the work and experiments that lead to this study. This project is made within the framework of a Marie Curie Industrial Host Fellowship (contract HPMI-CT-2002-00181).

References

[1] A. I. Schäfer, A. G. Fane, T. D. Waite, Nanofiltration principles and applications, Elsevier, Oxford, Chapters 1 and 21, (2005)

[2] W. R. Bowen, J. S. Welfoot, Modeling the performance of membrane nanofiltration-critical assessment and model development, Chem. Eng. Sci. 57 (2002) 1121-1137

[3] D. R. Machado, D. Hasson, R. Semiat, Effect of solvent properties on permeate flow through nanofiltration membranes. Part II Transport Model, J. Memb. Sci. 166 (2000) 63-69

[4] D. Bhanushali, S. Kloos, C. Kurth, D. Bhattacharyya, Performance of solvent-resistant membranes for non-aqueous systems: solvent permeation results and modeling, J. Memb. Sci. 189 (2001) 1-21

[5] D. Bhanushali, S. Kloos, D. Bhattacharyya, Solvent transport in solvent-resistant nanofiltration membranes for non-aqueous systems: experimental results and the role of solute-solvent coupling, J. Memb. Sci. 208 (2002) 343-359

[6] L. S. White, Transport properties of a polyimide solvent resistant nanofiltration membrane, J. Memb. Sci. 2005 (2002) 191-202

[7] B. vn der Bruggen, J. C. Jansen, A. Figoli, J. Geens, D. vn Baelen, E. Drioli, C. Vandecasteele, Determination of parameters affecting transport in polymeric membranes: Parallels between pervaporation and nanofiltration, J. Phys. Chem. B 108 (2004) 13273-13279

[8] J. Geens, K. Peeters, B. van der Bruggen, C. Vandecasteele, Polymeric nanofiltration of binary water-alcohol mixtures: influence of feed composition and membrane properties on permeability and rejection, J. Memb. Sci. 255 (2005) 255-264

[9] L. Braeken, B. Bettens, K. Boussu, P. van der Meeren, J. Cocquyt, J. Vermant, B. van der Bruggen, Transport mechanisms of dissolved organic compounds in aqueous solution during nanofiltration, J. Memb. Sci. 279 (2006) 311-319

[10] J. P. Robinson, E. S. Tarleton, C. R. Millington, A. Nijmeijer, Solvent flux through dense polymeric nanofiltration membranes, J. Memb. Sci. 230 (2004) 29-37

[11] R. Clément, A. Jonquières, I. Sarti, M. F. Sposata, M. A. C. Teixidor, P. Lochon, Original structure-property relationships derived from a new modeling of diffusion of pure solvents through polymer membranes, J. Memb. Sci. 232 (2004) 141-152

[12] A. Szymczyk, P. Fievet, Investigating transport properties of nanofiltration membranes by means of a steric and dielectric exclusion model, J. Memb. Sci. 252 (2005) 77-88

[13] J. A. Wesselingh, R. Krishna, Mass transfer in multicomponent mixtures, Delft University Press, Delft, (2000)

[14] J. M. K. Timmer, Properties of nanofiltration membranes; model development and industrial application, PhD thesis, Technische Universiteit Eindhoven, (2001), ISBN 90-386-2872-2

[15] G. D. C. Kuiken, Thermodynamics of irreversible processes, John Wiley and Sons, Chichester, (1994).

[16] E. Favre, P.Schaetzel, Q.T. Nguyen, R. Clément, J. Néel, Sorption, diffusion and vapor permeation of various penetrants through dense poly(dimethylsiloxane) membranes: a transport analysis, J. Membr. Sci. 92 (1992) 169-184

[17] M. V. Chandak, Y. S. Lin, W. Ji, R. J. Higgins, Sorption and diffusion of volatile organic compounds in polydimethylsiloxane membranes, J. Appl. Polym. Sci. 67 (1998) 165-175

[18] J. S. Vrentas, J. L. Duda, Diffusion in polymer – solvent systems. I. Reexamination of the free-volume theory, J. Polym. Sci. Part B: Polym. Phys. 15 (1977) 403-417

[19] J. S. Vrentas, J. L. Duda, Diffusion in polymer – solvent systems. II. A predictive theory for the dependence of diffusion coefficients on temperature, concentration and molecular weight, J. Polym. Sci. Part B: Polym. Phys. 15 (1977) 417-456

[20] P. B. Macedo, T. A. Litovitz, On the relative roles of free volume and activation energy in the viscosity of liquids, J. Chem. Phys. 42 (1965) 245-256

[21] P. J. A. M. Kerkhof, M. A. M. Geboers, Analysis and extension of the theory of multicomponent fluid diffusion, Chem. Eng. Sci. 60 (2005) 3129-3167

[22] J. Geens, Mechanisms and modeling of nanofiltration in organic media, PhD thesis, Katholieke Universiteit Leuven (2006) ISBN 90-5682-672-7

Chapter 3

Single-step retention analysis of solvent filtration by polymeric membranes

---

In this work a method is presented for the fast characterization of the separation performance of solvent resistant membranes. The method relies on the use of mass spectrometry and yields a full retention curve from a single retention experiment. Retention is based on the change in molecular weight (MW) distribution of a polyethylene glycol (PEG) solute between the feed and the permeate side. The method is independent of the solvent, resulting in a powerful tool for characterization of the multitude of non-aqueous filtration systems. The method has been applied to study the retention of a commercial nanofiltration membrane (Solsep 030206) in the filtration of methanol, 1-propanol and 1-pentanol. PEG with an average MW of 1000 Dalton has been selected as a solute. PEG is soluble in many relevant solvents, is readily available in a broad range of MW and does not present any health issues. In the case of 1-pentanol transport is mostly diffusive and the solute is completely retained. In contrast, for methanol and 1-propanol solvent transport is much faster and dragging effects cause smaller PEG oligomers to be transported through the membrane. The molecular weight cut-off (MWCO) is similar for both methanol and 1-propanol, i.e. 900 Da, although the hydrodynamic radius of the solute is bigger in methanol when compared to 1-propanol.

3.1 Introduction

In membrane filtration retention is generally quantified based on the size or MW of a solute that is retained by the membrane. Various techniques are available for retention studies, including the simple determination of the molecular weight cut-off (MWCO). For microfiltration and ultrafiltration, pores have been well defined in literature and the properties of the solvent and solute can be extrapolated from the liquid bulk to the inside of the pores [1-4]. This for instance allows the use of the hydrodynamic volume of the solute in the bulk to quantify the pore dimensions [5]. For systems in which the pore size is comparable to the dimensions of the permeating molecules, in particular in the nanofiltration range, interpretation of retention data is less straightforward. This becomes more complex when non-aqueous solvents are involved. For these systems many variables are not well-defined or understood, for instance: pore morphology, swelling and compaction phenomena, transport mechanisms and specific (competitive) interactions between the solvent, solute and membrane. This impairs applicability of existing retention characterization methods. Moreover, literature shows that the large number of variables demands independent studies for essentially each distinct solvent/membrane system [6-11]. For this reason new methods are required that allow fast and straightforward retention studies in different solvent environments.

In literature a method has been presented where styrene oligomers are used as solutes for the characterization of the MWCO of a commercial membrane [12]. The method yields a retention curve from a single experiment, but is limited to solvents in which styrene oligomers are sufficiently soluble. In this work we will show that a retention curve can be obtained using a low concentration of a solute with a broad MW distribution. The low concentration of the solute aids in overcoming limitations related to solubility. Using mass spectrometry allows accurate quantification of very low concentrations (ppm) of the solute. Coupling the mass spectrometer with liquid chromatography enables monitoring the change in the distribution of the MW between the retentate and the permeate. In this way only a single experiment is required to obtain a full retention curve. For this purpose, PEG with an average MW of 1000 Da has been selected. This solute is sufficiently soluble in many solvents, is inexpensive, readily available in different

ranges of MW and does not present any health hazards [13]. The method is applied to a commercially available solvent resistant nanofiltration (SRNF) membrane (Solsep 030206) in the filtration of methanol, 1-propanol and 1-pentanol. The retention results are analyzed in terms of MWCO and solute hydrodynamic size.

3.2 Method

The solute used (PEG) has been selected based on the broad MW distribution (from 600 to 1300 Da). This property will be used to obtain a retention curve based on one single experiment. The initial concentration of solute in the feed solution is kept low (200 to 300 ppm), to ensure that the solubility of the solute is not an issue. For each oligomer *i* the solute retention is defined according to Equation 3.1

$$R_i = 1 - \frac{C_{i,P}}{C_{i,R}} \qquad (3.1)$$

where C is the concentration in the permeate (P) or in the retentate (R). During sample preparation, known amounts of sample are taken from the retentate and permeate. Subsequently, the solvent is evaporated in a vacuum oven and replaced by water. This renders the analysis solvent independent. Retention becomes

$$R_i = 1 - \frac{C'_{i,P}}{C'_{i,R}} \frac{\varphi_P}{\varphi_R} \qquad (3.2)$$

Here C is the weight concentration of the oligomer in the aqueous samples. The solvent exchange factor

$$\varphi = \frac{n_w}{n_s} \qquad (3.3)$$

represents the ratio of the mass n_s of solvent exchanged by a mass n_w of water. The concentration C'_i is determined using liquid chromatography, coupled to a mass spectrometer (LC-MS). LC

separates the oligomers based on the corresponding residence time in the column. Each oligomer is then ionized in the MS, resulting in a mass/charge ratio spectrum. The same oligomer is represented by several ionization peaks in the spectrum. The quantity of the oligomer can be directly related to the sum of the peak areas (A_i). By approximation, the quantity can be assumed proportional to the sum of the peak areas.

$$C_i^{'} = K_i A_i \qquad (3.4)$$

Substitution of Equation 3.4 in Equation 3.2 yields the following equation for the retention

$$R_i = 1 - \frac{A_{i,P}}{A_{i,R}} \frac{\varphi_P}{\varphi_R} \qquad (3.5)$$

Note that this expression is independent of the linear response factor K_i.

3.3 Experimental

A commercial membrane was used, Solsep 030206 from Solsep, the Netherlands. Methanol (99%), 1-propanol (99%), 1-pentanol (99%) and PEG 1000 were obtained from Sigma-Aldrich. All the retention experiments were performed in a batch membrane module (Figure 3.1). The membrane had an effective area of 56.75 cm^2, maximum feed volume of 650 mL and a limiting pressure of 65 bar controlled by a relief valve. The feed solutions were prepared for a maximum starting concentration of 300 ppm of PEG in each of the alcohols. The membranes used in the experiments were previously swollen for a period of 2 days. Before the first experiment, the membrane was compacted to a maximum working pressure of 40 bar, in order to reduce the influence of compacting effects during experiments. All experiments were performed at a constant transmembrane pressure of 30 bar. Because sampling was not possible while the module is pressurized, samples of the feed solution were taken before the start of the experiment.

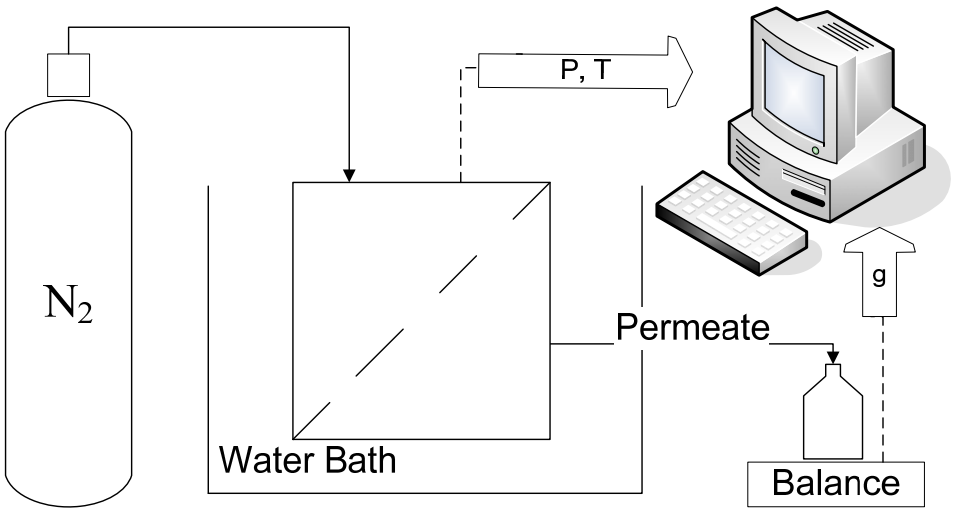

Figure 3.1: Schematic representation of the batch permeation set-up.

After a small amount (50 mL) of permeate was recovered, samples were taken directly from the permeate stream to determine retention. LC-MS measurements were performed using a LC-10ADVP pump, supplied by Shimatzu and an auto-sampler Surveyor from Thermo Finnigan. The LC column was an Alltima HP C8 3µ with a liquid flow rate of 0.2 mL/min. The mass spectrometer was supplied by Thermo Finnigan LCQ, Deca Xp max.

3.4 Results and discussion

3.4.1 LC-MS accuracy/analysis

Figure 3.2 depicts the relation between the concentration of different PEG molecules in an aqueous solution and the sum of their peak areas resulting from LC-MS analysis. Clearly, for the different oligomers the assumption of a linear response (Equation 3.4) is valid. The effect of replacing the solvent in the samples with water is depicted in Figure 3.3. The closed dots in this figure represent the total solute concentration of samples prepared directly with water. The open dots represent samples prepared using the solvent exchange procedure, i.e. where 1-propanol is

replaced by water. Clearly, the total solute concentration is not significantly affected by the solvent exchange procedure.

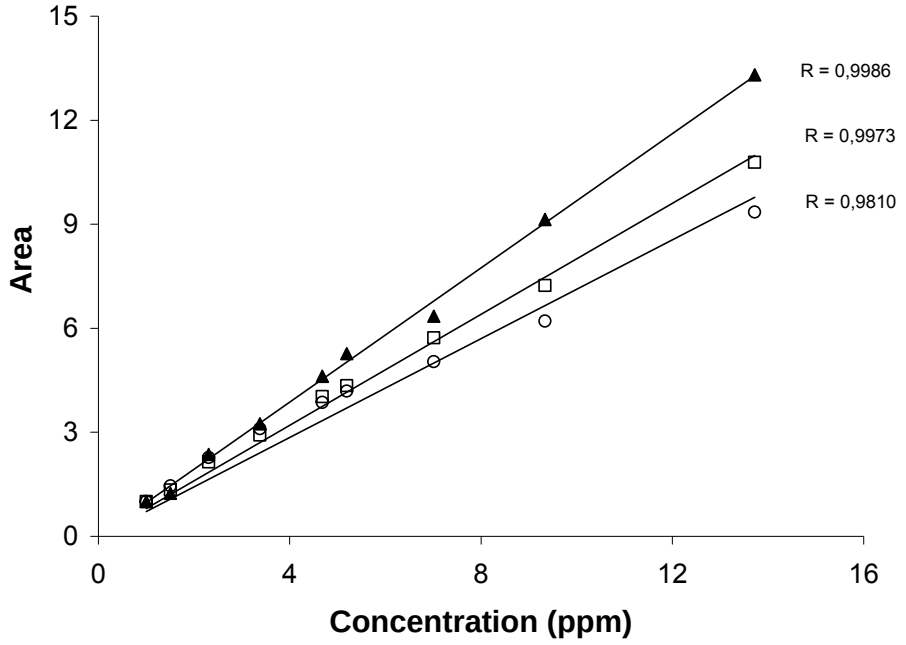

Figure 3.2: Concentration vs. MS area peak for (□) PEG 722 Da, (o) PEG 1030 Da and (▲) PEG 1338 Da.

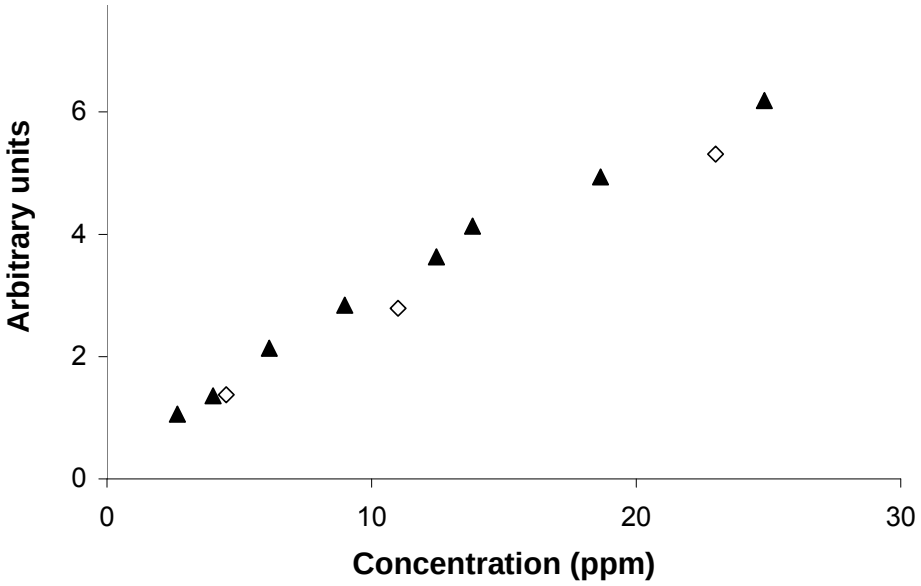

Figure 3.3: (▲) Calibration line using samples prepared directly with water; (◊) samples prepared using 1-propanol and submitted to solvent exchange procedure.

3.4.2 Membrane performance

Figure 3.4 shows the flux observed during a retention experiment for the case of 200 ppm of PEG in 1-propanol and in 1-pentanol. The flux observed for 1-propanol is stable throughout the experiment, whereas the flux of 1-pentanol is extremely low and can be considered zero within experimental error. The flux of methanol (Figure 3.5) is higher and shows a decrease in time.

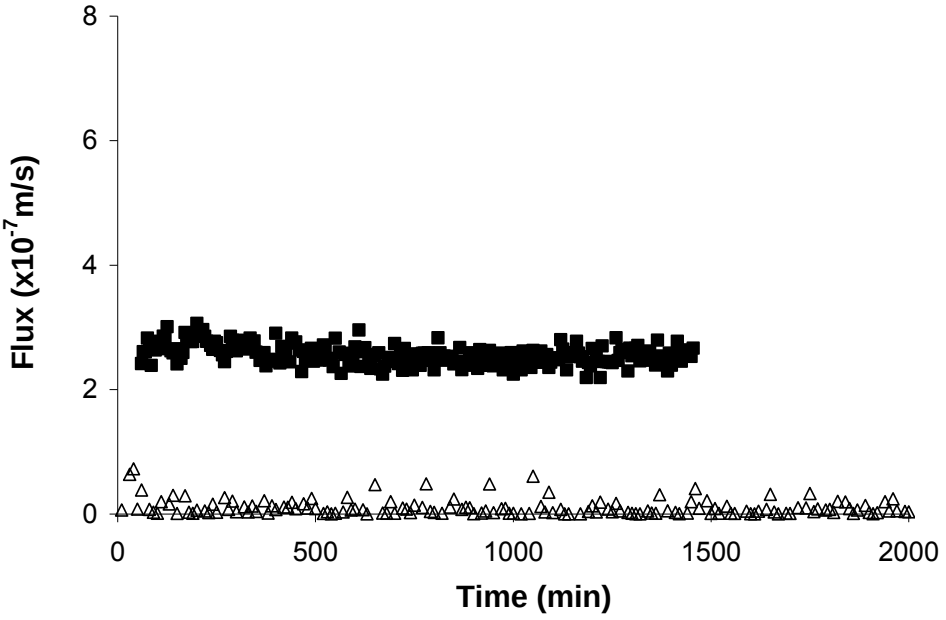

Figure 3.4: Retention experiments using a Solsep 030206 performed with a solution of 200 ppm of polyethylene glycol in (■) 1-propanol and (Δ) 1-pentanol. Flux measurements performed at a transmembrane pressure of 30 bar and a temperature of 20 ºC.

In the case of methanol, the duration of the experiment is restricted by the limited volume of the batch module. The decreasing flux of methanol can not be related to osmotic effects, as the solute concentration in the module is kept at a very low value (max. 1500 ppm). In addition, the Peclet number of this system equals unity (Pe = 1) where concentration polarization effects are negligible [14, 15]. Also because the concentration of PEG is so low, accumulation of PEG molecules in the matrix is not likely to be the cause of the decreasing flux.

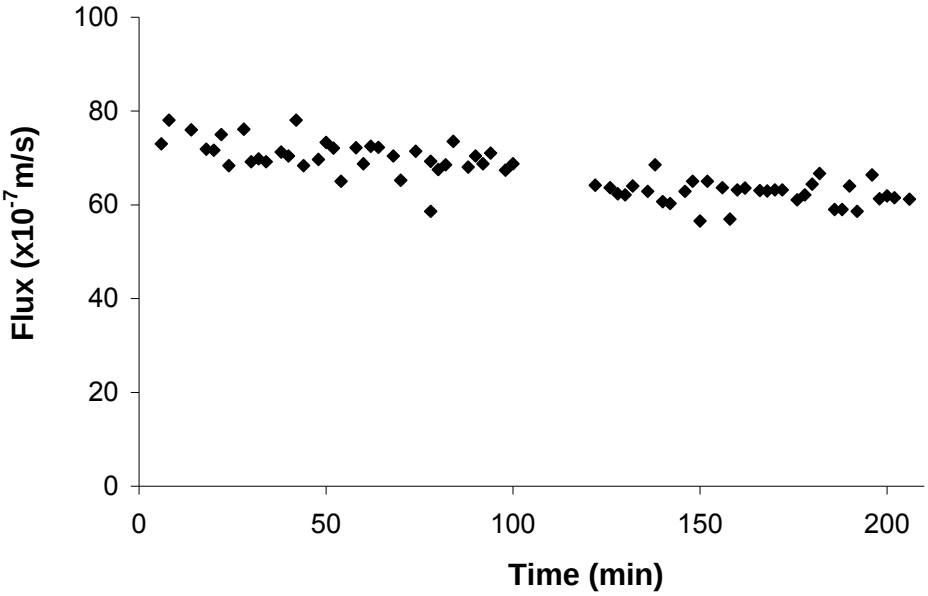

Figure 3.5: Retention experiment using a Solsep 030206 performed with a solution of 200 ppm of polyethylene glycol in (♦) methanol. Flux measurements performed at a pressure of 30 bar and a temperature of 20 ºC.

Previous experiments have shown that flux of faster permeating molecules such as methanol but also ethanol are less stable. The origin of this behavior is probably related to compaction and swelling effects. These phenomena have a stronger influence on viscous transport as compared to diffusive transport. This will be discussed more elaborately in Chapter 6.

3.4.3 Retention performance

Figure 3.6 shows the retention of different oligomers as a function of MW, for the three different alcohols at room temperature. Retention is high in 1-pentanol (above 95%) when compared to methanol and 1-propanol. The difference is more pronounced for lower MW. The high retention in the case of 1-pentanol is due to the low flux of this solvent. 1-Pentanol transport is mainly dominated by diffusion, as it has been discussed in Chapter 1. Due to the low transport rate there is no significant dragging effect that will enhance the transport of PEG molecules. As a consequence, all PEG molecules will slowly diffuse through the membrane. In the case of methanol and 1-propanol a lower retention is observed for the smaller PEG oligomers.

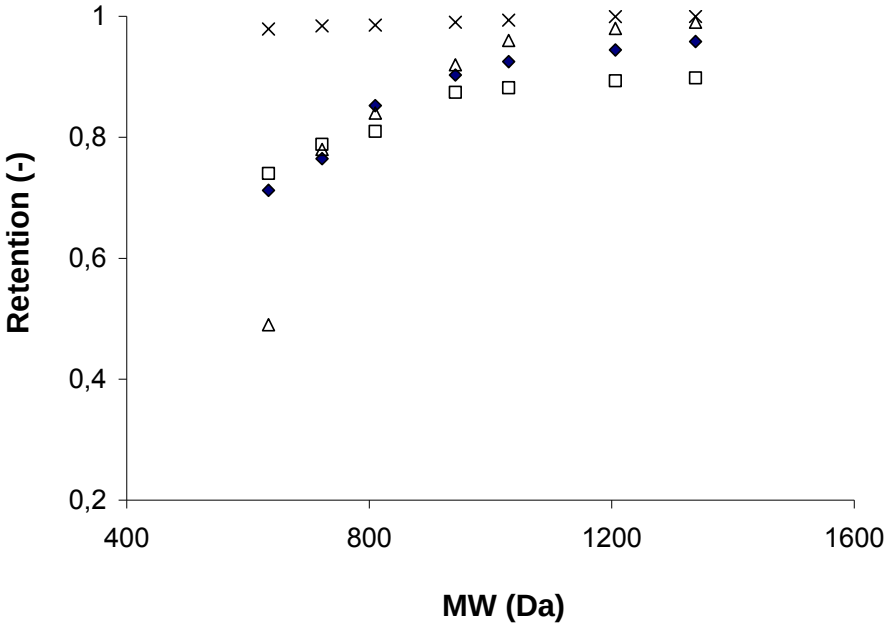

Figure 3.6: Retention of several PEG oligomers by a Solsep 030206 membrane in (◆,□) methanol, (Δ) 1-propanol and (x) 1-pentanol at 30 bar and 20 ºC.

The lower retention is due to much higher solvent fluxes as compared to 1-pentanol. For methanol and 1-propanol dragging effects are expected that will lead to a strong increase of the PEG transport rate, especially for the smaller oligomers. The resulting MWCO corresponding to 90% retention is similar for methanol and 1-propanol (Table 3.1).

Solvent	R (%)	MWCO (Da)
Methanol	90	942
1-Propanol	90	894
1-Pentanol	90	<600

Table 3.1: Retention of PEG and MWCO resulting from the retention experiment performed with 200 ppm of PEG in methanol, 1-propanol and 1-pentanol.

The similar retention values for methanol and 1-propanol are unexpected because the methanol flux is much higher. However, it should be taken into consideration that the size and shape of the solute is different in the two solvents. In Figure 3.7 the hydrodynamic radii of PEG oligomers are plotted for different solvents. The graph shows that in a bulk solution all oligomers have a radius below 10 Å. The same PEG oligomer has a different radius in different solvents. For example, PEG 600 has a radius of 7 Å in methanol and 5.5 Å in 1-pentanol.

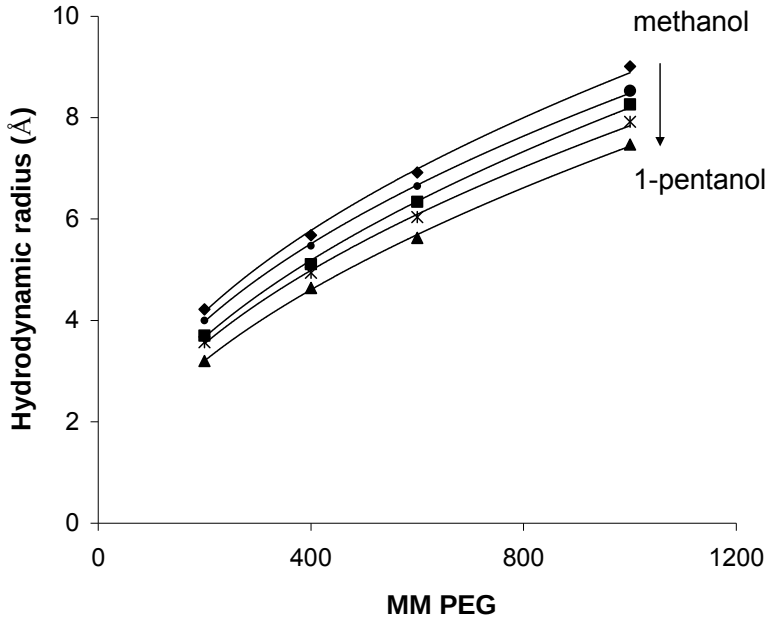

Figure 3.7: Hydrodynamic radius of PEG in: (◆) methanol; (●) ethanol; (■) 1-propanol; (∗) 1-butanol and (▲) 1-pentanol at 20 ºC, determined from the one-point method [16, 17].

In Figure 3.8 the retention is plotted as a function of the hydrodynamic radii of the PEG oligomers in the bulk solution. For PEG oligomers of similar size, retention is lower in the case of methanol as compared to 1-propanol. The difference in retention is related to the solvents transport rates, as is confirmed by the high retention observed for the slowly diffusing 1-pentanol. Clearly, the retention results can not solely be interpreted in terms of size or shape of the solute; the rate and mechanism of the solvent transport have to be taken into account also.

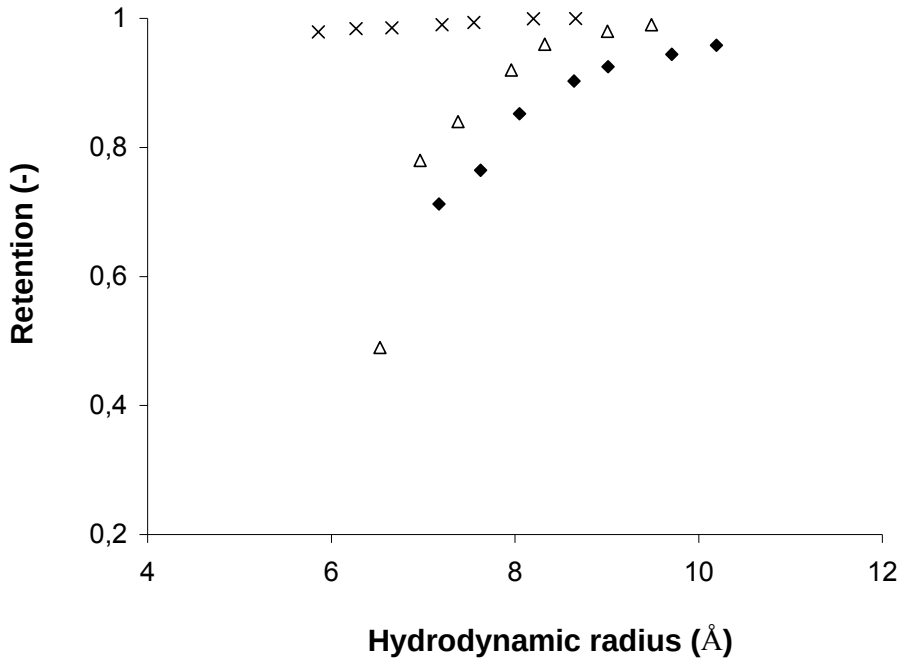

Figure 3.8: Retention of several PEG oligomers by a Solsep 030206 membrane in (◆) methanol, (Δ) 1-propanol and (X) 1-pentanol at 30 bar and 20 ºC

3.5 Conclusions

A generic method is presented that allows determination of the retention behavior in non-aqueous solvent filtration. The method has no restrictions with respect to solute solubility and is independent of the solvent studied. Using a low concentration of one solute with a broad MW distribution, combined with a powerful analytical technique, a single retention experiment produces a full retention curve. This way, the MWCO of the membrane in the solvent can be directly determined and the cost and time of the experimental procedure is reduced. The value of such a method resides in the existence of a multitude of systems, in particular in the application of polymeric nanofiltration membranes to solvent recovery.

The retention of PEG 1000 has been determined for a commercial membrane. Retention is mostly dependent on the rate and mechanism of solvent transport. For methanol and 1-propanol, where transport is solely or partially determined by viscous transport, dragging effects cause the retention of small PEG oligomers to be low, and a 90% MWCO of 900 Da is observed. Although

the MWCO is similar for both solvents, the size of the PEG oligomers is dependent on the solvent environment. Oligomers with similar dimensions show lower retention in the case of the solvent with the highest flux, i.e. methanol. In the case of 1-pentanol solvent transport is primarily determined by diffusion and dragging effects are insignificant. Consequently, PEG oligomers only permeate through the membrane by diffusion and retention is high, irrespective of the size and shape of the solute molecule.

Acknowledgements

We would like to thank Monique Dohmen for all the experimental work that lead to this study. This project is made within the framework of a Marie Curie Industrial Host Fellowship (contract HPMI-CT-2002-00181).

References

[1] R. Nobrega, H. Balmann, P. Aimar, V. Sanchez, Transfer of dextran through ultrafiltration membranes: a study of rejection data analyzed by gel permeation chromatography, J. Memb. Sci. 45 (1989) 17-36

[2] G. Schock, A. Miquel, R. Birkenberger, Characterization of ultrafiltration membranes: cut-off determination by gel permeation chromatography, J. Memb. Sci. 41(1989) 55-67

[3] P. Aimar, M. Meireles, V. Sanches, A contribution of the translation of retention curves into pore size distributions for sieving membranes, J. Memb. Sci. 54 (1990) 321-338

[4] M. Meireles, P. Aimar, V. Sanchez, Effects of protein fouling on the apparent pore size distribution of sieving membranes, J. Memb. Sci. 56 (1991) 13-28

[5] M. Meireles, A. Bessieres, I. Rogissart, P. Aimar, V. Sanchez, An appropriate molecular size parameter for porous membranes calibration, J. Memb. Sci. 103 (1995) 105-115

[6] N. Stafie, D. F. Stamatialis, M. Wessling, Effect of PEDMS crosslinking degree on the permeation performance of PAN/PDMS composite nanofiltration membranes, Sep. Purif. Technol. 45 (2005) 220-231

[7] J. Geens, K. Peeters, B. van der Bruggen, C. Vandecasteele, Polymeric nanofiltration of binary water-alcohol mixtures: Influence of feed composition and membrane properties on permeability and rejection, J. Memb. Sci. 255 (2005) 255-264

[8] J. Geens, A. Hillen, B. Bettens, B. van der Bruggen, C. Vandecasteele, Solute transport in non-auqueous nanofiltration: effect of membrane material, J. Chem. Technol. Biotechnol. 80 (2005) 1371-1377

[9] I. F. J. Vankelekom, K. D. Smet, L. E. M. Gevers, A. Livingston, D. Nair, S. Aerts, S. Kuypers, P. A. Jacobs, Physico-chemical interpretation of the SRNF transport mechanism for solvents through dense silicone membranes, J. Memb. Sci. 231 (2004) 99-108

[10] L. G. Peeva, E. Gibbins, S. S. Luthra, L. S. White, R. P. Stateva, A. G. Livingston, Effect of concentration polarization and osmotic pressure on flux in organic solvent nanofiltration, J. Memb. Sci. 236 (2004) 121-136

[11] E. S. Tarleton, J. P. Robinson, C. R. Millington, A. Nijmeijer, Non-aqueous nanofiltration: solute rejection in low-polarity binary systems, J. Memb. Sci. 252 (2005) 123-131

[12] Y. H. See Toh, X. X. Loh, K. Li, A. Bismarck, A. G. Livingston, In search of a standard method for the characterization of organic solvent nanofiltration membranes, J. Memb. Sci. 291 (2007) 120-125

[13] http://www.ilo.org/public/english/protection/safework/cis/products/icsc/dtasht/index.htm (2006)

[14] C. Causserand, S. Rouaix, A. Akbari, P. Aimar, Improvement of a method for the characterization of ultrafiltration membranes by measurements of tracers retention, J. Memb. Sci. 238 (2004) 177-190

[15] J. G. Wijmans, A. L. Athayde, R. Daniels, J. H. Ly, H. D. Kamaruddin, I. Pinnau, The role of boundary layers in the removal of volatile organic compounds from water by pervaporation, J. Memb. Sci. 109 (1996) 135-146

[16] O. F. Solomon, I. Z. Ciuta, Determination de la viscosité intrinsèque de solutions de polymers par une simple determination de la viscosité, J. Appl. Polym. Sci. 24 (1962) 683-686

[17] A. Rudin, R. A. Wagner, A new one-point intrinsic viscosity method, J. Appl. Polym. Sci. 19 (1975) 3361-3367

Chapter 4

Solvent sorption measurements in polymeric membranes with ATR–IR spectroscopy

Long-term stability and performance of polymeric membranes in solvent and mixed solvent media can be reduced due to sorption and swelling of the membrane matrix. For this reason quantification of sorption and swelling is of major importance for the development of future applications of membrane processes in solvent and mixed solvent media. In this work a method is discussed, based on attenuated total reflectance infrared spectroscopy (ATR-IR), to establish sorption and sorption selectivity of a cellulose acetate (CA) membrane in water/methanol and water/ethanol mixtures. By analysis of specific peaks from the ATR-IR spectra of the solvents, the preferential sorption of water in CA membranes can be quantified. In the presence of methanol, the selectivity for water ranges from 2.5 to 3.5 between 52% and 90% of methanol. For ethanol, the selectivity for water ranges from approximately 1 (30% ethanol) to 2 (90% ethanol). From the work it follows that ATR–IR provides an easy and non-destructive method to study the sorption behavior of the active layer of the membrane.

4.1 Introduction

Since industry uses large amounts of solvents, about 4.3 million tonnes annually in Europe [1], the need for technology to insure re-use is becoming increasingly important. Many examples in the food and pharmaceutical industry have shown that membrane processes can substantially decrease the energy consumption for separations involving aqueous streams [2]. However, the application of membrane technology for the separation of solvent and mixed solvent media streams is still rather limited despite the potential reduction in costs. This is due to the fact that long-term stability and performance of polymeric membranes in solvent and mixed solvent media is often unknown and is still in a very early stage of study. Therefore, it is important to understand phenomena like swelling and sorption that contribute to a reduction of the life-time of the membrane. Several techniques are available to study sorption and swelling of polymers and an overview is presented in Figure 4.1 [3].

Studies based on weight measurements do not take into account that in supported films the swelling and sorption is not the same at both sides of the membrane. The need for a separate sample of active polymeric layer increases cost and time spent on the study and is often impossible for commercial samples. Techniques for the measurement of parallel elongation and thickness dilation of a film are very demanding in terms of experimental set-up and also require separate samples of the active layer. As an example, sorption and longitudinal swelling kinetics of the system CA and methanol have been studied by Sanopoulo [4] using a differential swelling stress model (LDSS). Methanol was found to be a weak swelling agent and the interactions with the CA structure preferentially occur with the hydroxyl groups.

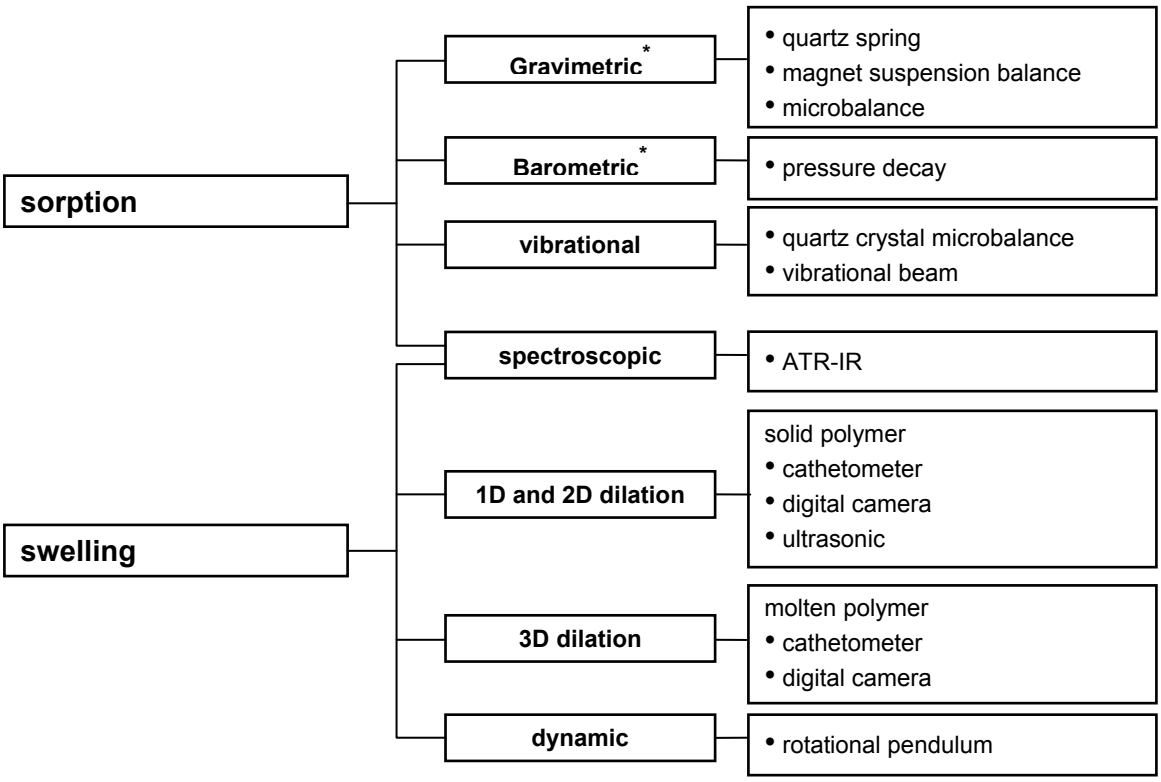

Figure 4.1: Overview of sorption and swelling measurement methods. * These methods require additional swelling data. (Reproduced with permission [2]).

With the use of ATR-IR the active layer of a membrane can be analyzed without the need of a destructive sample preparation. ATR-IR has been used under supercritical conditions ($scCO_2$), underlining the possibilities of simultaneously measuring sorption and swelling of the polymer used [5-9]. Some literature has also been published on diffusion in thin polymer films [10, 11]. The results show that in combination with an appropriate diffusion model, it is possible to use ATR-IR to study diffusion. These studies also show that the measurements can be obtained in a gaseous or liquid phase opening the possibility to use the same technique in the characterization of polymeric membranes. Currently, ATR-IR is used to identify surface changes and the presence of impurities in polymeric membranes [12]. Freger and Belfer have used ATR-IR to study surface changes in polyamide membranes due to grafting [13] and fouling of membranes by proteins [14, 15]. The ability to differentiate between parallel and perpendicular polarized light in ATR-IR

[16] allows the study of the alignment of molecules at the surface of hollow fiber membranes [17].

In this work we explore the use of ATR-IR as a non-destructive method to study preferential sorption in commercial polymeric membranes in the presence of organic solvents. As a model system, we have used cellulose acetate membranes in combination with aqueous methanol and ethanol solutions.

4.2 Theory

ATR-IR spectroscopy is based on total reflection of the infrared (IR) beam (Figure 4.2).

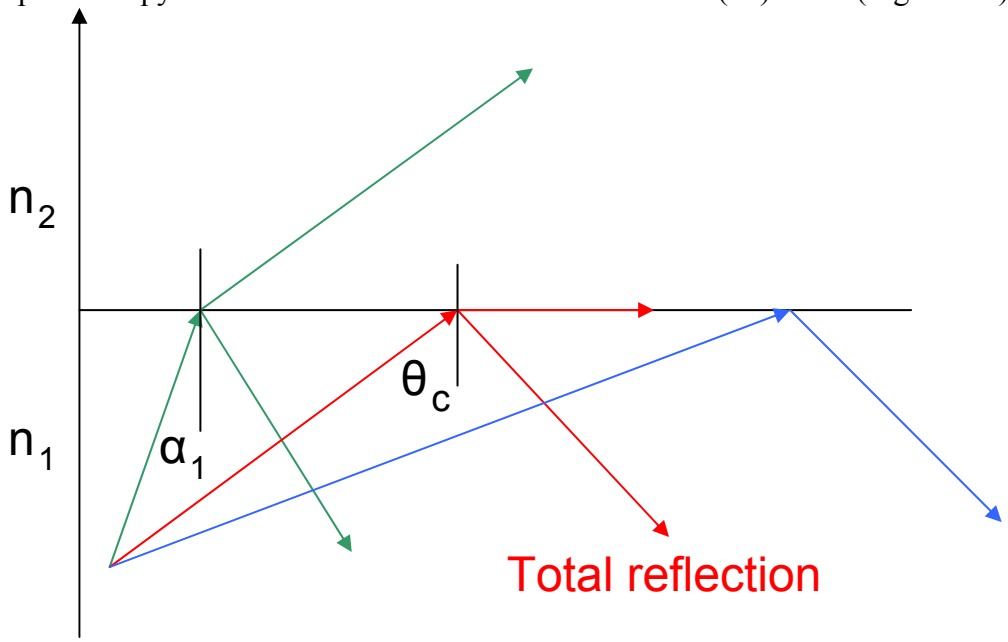

Figure 4.2: Effect of angle of incidence on direction of the IR beam propagation.

In order to have internal reflection, the refractive index of the sample (n_2) must be lower than the refractive index of the crystal (n_1). The region of total reflection begins at an angle higher than a critical angle (θ_c) calculated for a reflectance angle (α_2) of 90 degrees, using Snell's Law (Equation 4.1):

$$\sin\theta_c = \frac{n_2}{n_1} \qquad (4.1)$$

where n_1 is the refractive index of the ATR-IR crystal and n_2 the refractive index of the sample. In this region of reflection all the information from the sample (functional group vibrations) can be detected by the spectrometer. With ATR-IR spectroscopy, one important aspect to take into account is the depth of penetration (dp) of the IR beam (Equation 4.2). This value depends on several factors and can be calculated from the following equation:

$$dp = \frac{\lambda}{2\pi(n_1^{\,2}\sin^2\theta - n_2^{\,2})^{1/2}} \qquad (4.2)$$

where θ is the incidence angle and λ is the wavelength of the incident beam. This value becomes critical when the sample is a membrane with an active layer in the range of 1 to 10 μm. The possibility of changing dp by changing the crystal used makes ATR–IR an ideal technique for analysis and characterization of thin layer polymer membranes [16].

However, quantification in ATR-IR spectroscopy is still not as straightforward as in transmittance spectroscopy. Each peak in ATR-IR relates to a determined amount of energy absorbed by a specific functional group present in the sample. The resulting energy (peak absorbance) is a result of several scans performed by the spectrometer and, therefore, is not an exact concentration but rather a statistical measure.

In this study sorption of methanol, ethanol and water in CA membranes is studied. Sorption is related to the peak area and the sorption selectivity of a membrane can be expressed by the selectivity parameter (α):

$$\alpha = \frac{\left(C_{w,m} / C_{s,m}\right)}{\left(C_{w,f} / C_{s,f}\right)} \qquad (4.3)$$

where $C_{w,m}$ and $C_{w,f}$ is the concentration of water in the membrane and in solution, respectively, and $C_{s,m}$ and $C_{s,f}$ is the concentration of methanol or ethanol in the membrane and in solution, respectively.

4.3 Experimental

The membrane used was a polymeric flat sheet 3 kD CA membrane provided by Microdyn-Nadir filtration GmbH, Germany. Methanol (99.9%) and ethanol (99.9%) were obtained from Sigma-Aldrich. Experiments were performed with solutions of different concentrations of alcohol in a range from 0 to 100% (w/w).

4.3.1 ATR–IR spectra

The ATR-IR spectra were recorded with a Nicolet Protege 460 Fourier-Transform infrared spectrometer with Nicolet Smart Golden Gate Mk II total reflectance device using a diamond crystal at an incidence angle of 45º. Each spectrum results from 32 scans at 4 cm^{-1} resolution for a spectral range from 4000 to 650 cm^{-1}. The penetration depth of the IR beam in the CA membrane sample was calculated to be between 0.9 and 1 μm at 2000 cm^{-1}. All the readings were performed at room temperature. Based on statistical calculations performed at the beginning of this study for a measurement error lower than 5% in each area value obtained, 10 spectra of the same sample were always recorded. In the spectra taken of methanol, ethanol, water and CA, specific peaks were identified and the increase in area of these peaks is used for sorption calculations. In the case of overlapping peaks, deconvolution was performed for the calculation of the contribution of the individual peaks using Origin 6.0 software from Microcal.

4.3.2 Sample preparation

Each sample of CA membrane was brought in contact with the alcohol solution for one hour. This time was based on previous experiments in order to guarantee equilibrium. In order to determine the thickness of the active layer of the dry membrane, Scanning Electron Microscopy (SEM) pictures were taken of the CA membranes using a JEOL 840 microscope. The pictures

show an active layer with a thickness of 3 μm (Figure 3), which is more than the penetration depth of the IR beam, thus fulfilling the requirement to apply ATR-IR spectroscopy.

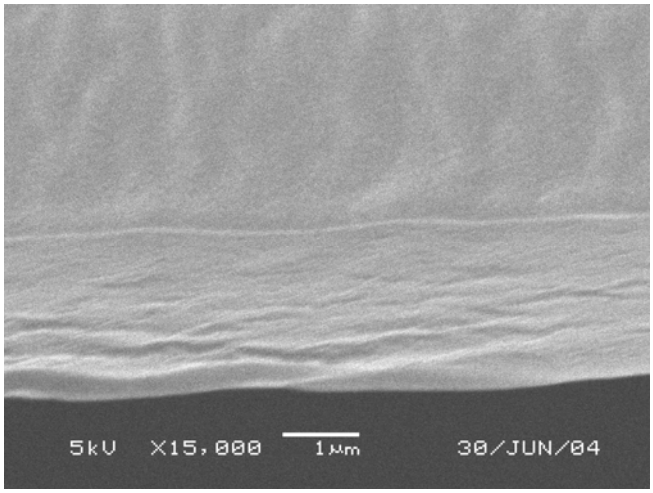

Figure 4.3: SEM micrographs of the active layer of the cellulose acetate membrane.

In order to study the variability of the CA membrane material, two sets of 5 membrane pieces were placed in water for the period of one hour. In the first set of experiments, the ATR-IR readings were performed at 10 different locations of the membrane for each of the 5 samples. In the second set of experiments, the 10 readings were performed at exactly the same spot of the membrane for each of the 5 samples.

4.4 Results and discussion

4.4.1 Peak identification

The specific peaks of methanol, ethanol, water and CA membrane are identified in Figure 4.4.

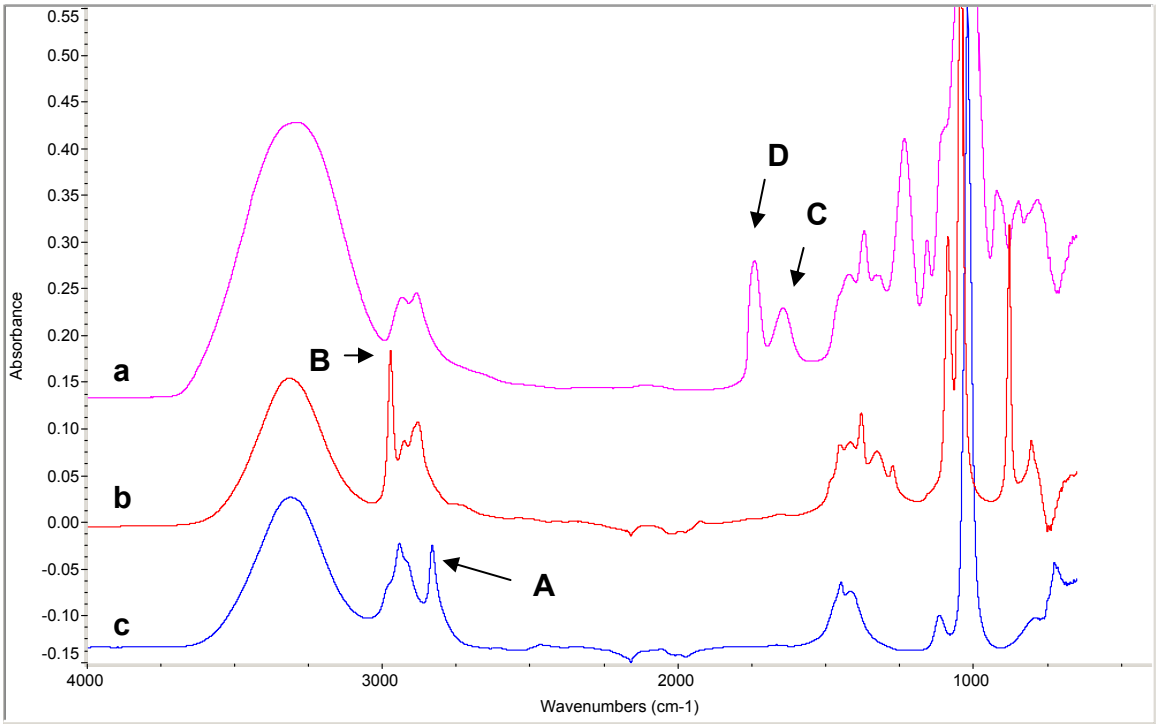

Figure 4.4: ATR–IR spectra of (a) cellulose acetate, (b) ethanol and (c) methanol. The specific peaks are identified as: (A) – methanol; (B) - ethanol; (C) – water; (D) – cellulose acetate, carbonyl group vibrations.

The specific peak of methanol (A) refers to the vibration of the methyl group (CH_3) absorbing at 2831 cm^{-1}. For ethanol (B) the specific vibration is common for all primary alcohols, with the exception of methanol, where a peak appears at 2972 cm^{-1} due to the CH_2 group vibration. The peak related to the presence of water (C) in the sample has a specific vibration at 1639 cm^{-1} [18]. The CA membrane has a specific peak (D) related to the vibration of the carbonyl group at 1736 cm^{-1}. For pure cellulose acetate a water peak would not be expected. However, it appeared to be impossible to remove the water present in the commercial sample as the polymeric structure changes and becomes damaged once dried.

4.4.2 Peak deconvolution

From Figure 4.4 it is evident that the specific peak of methanol (A) overlaps with the peak in spectrum (a) resulting from vibration of the CH, CH_2 and CH_3 groups in the CA membrane structure (2930 cm^{-1} and 2886 cm^{-1}). The same occurs for the ethanol specific peak (B) for the first two vibrations. Deconvolution is used to estimate the area related to the specific vibration of the desired peak (A or B) only and no distinction is made between the CH and CH_2 contribution to the peak from the CA membrane. It appeared to be impossible to obtain reliable deconvolution values for the area of the methanol peak for concentrations lower than 50%. For ethanol, deconvolution is possible for concentrations higher than 30%.

4.4.3 Solution readings – trend line

The ATR-IR spectra taken of the solutions used in the experiments show an increase of the peak absorbance with increasing concentration (Figure 4.5).

a)

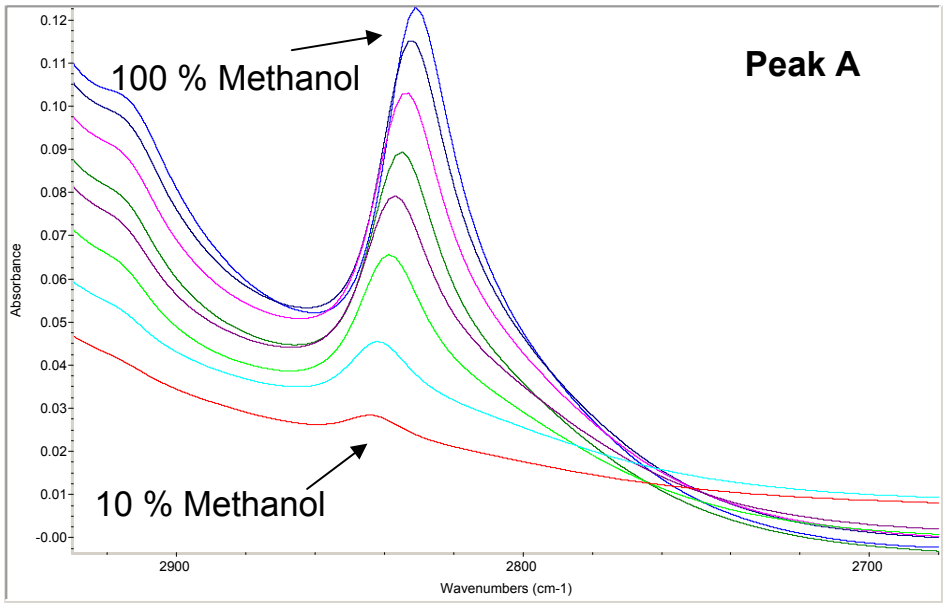

b)

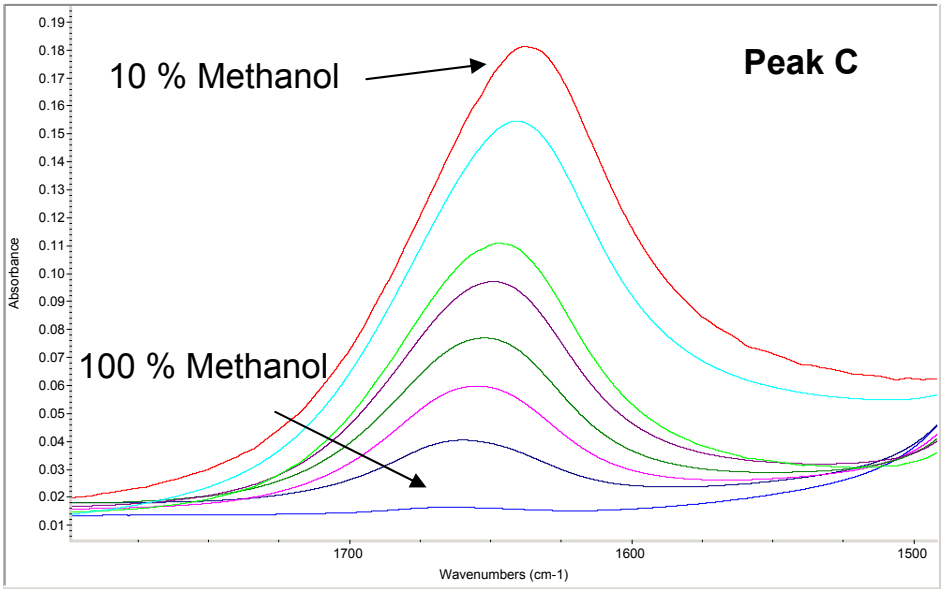

Figure 4.5: Gradual increase/decrease of the specific peak of a) methanol and b) water with the increase in methanol concentration.

As can be seen from Figure 4.6, the peak area versus the concentration of methanol, ethanol or water in solution shows an almost linear relation. Also, for overlapping peaks like the methanol or ethanol specific peak, the error of the area reading becomes somewhat higher as compared to the peak of water. However, these results show that ATR-IR allows for quantification of the concentration of the solvent. Performing 10 consecutive spectral readings at the same location of the membrane leads to an accuracy in the measurement of about 5%. However, performing the measurements on different pieces of membrane leads to an accuracy of approximately 15%. This decreased accuracy is probably due to the structural inhomogeneity of a membrane sheet, leading to a variation of the free volume of the polymer matrix along the membrane surface.

a)

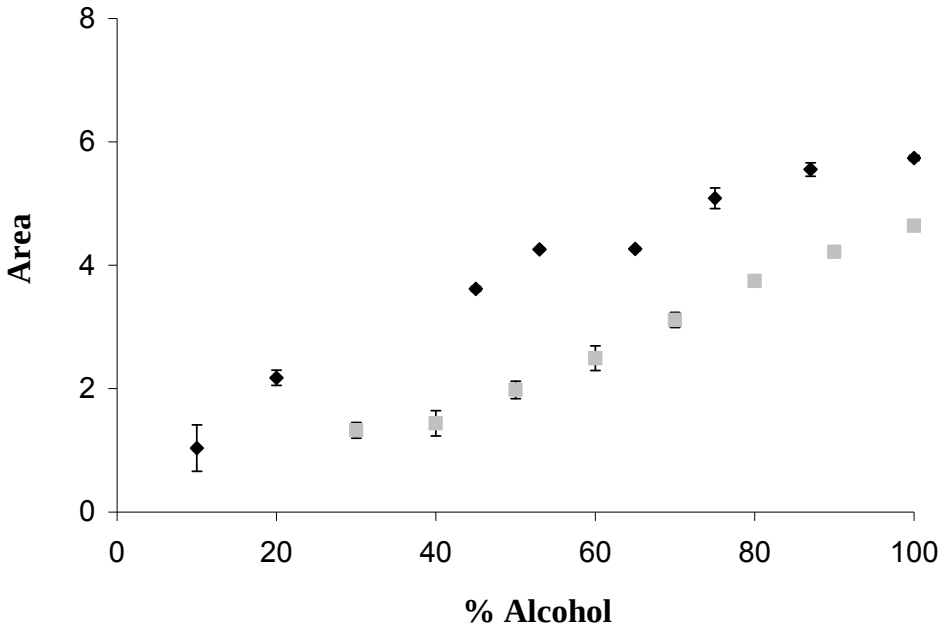

b)

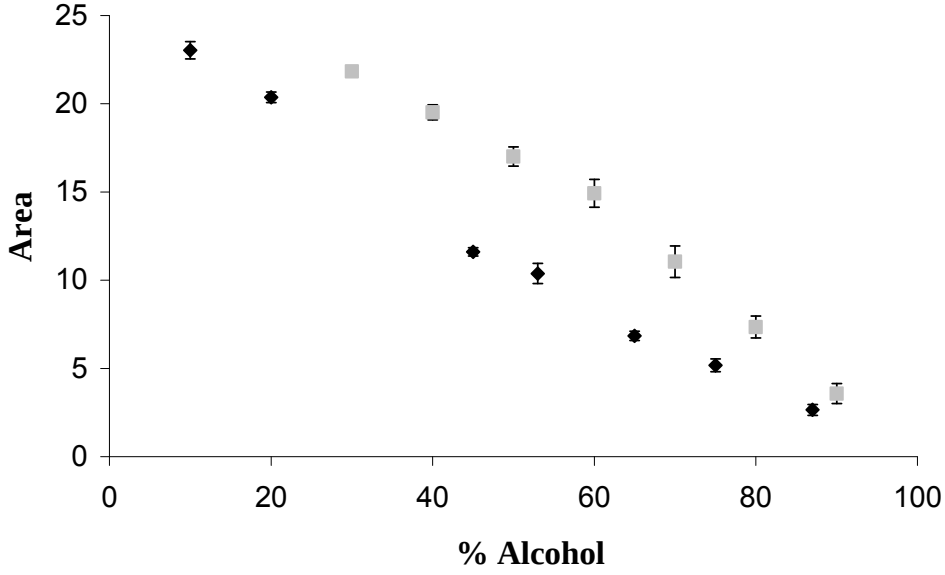

Figure 4.6: Alcohol solution readings: a) Gradual change of methanol (◆) and ethanol (■) specific peak area with solution concentration; b) gradual change of water specific peak area in methanol (◆) and ethanol (■) solutions.

4.4.4 Change in peak wavenumber

The methanol peak area (peak A) and the ethanol peak area (peak B) not only increase with increasing concentration but also the frequency at which the specific group absorbs energy shows a decrease (Figure 4.7).

a)

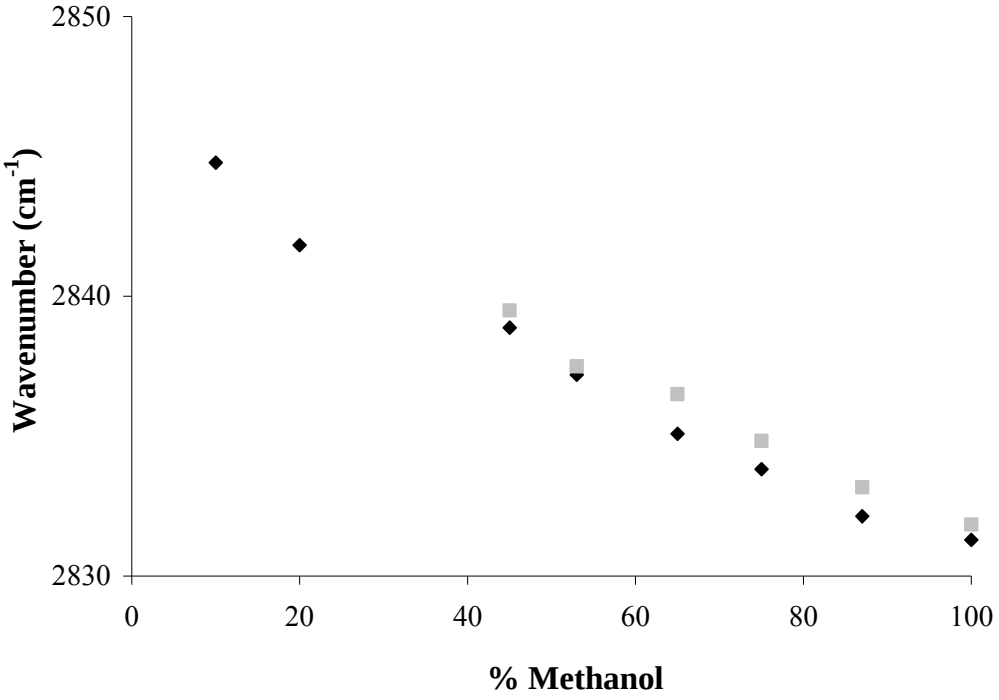

b)

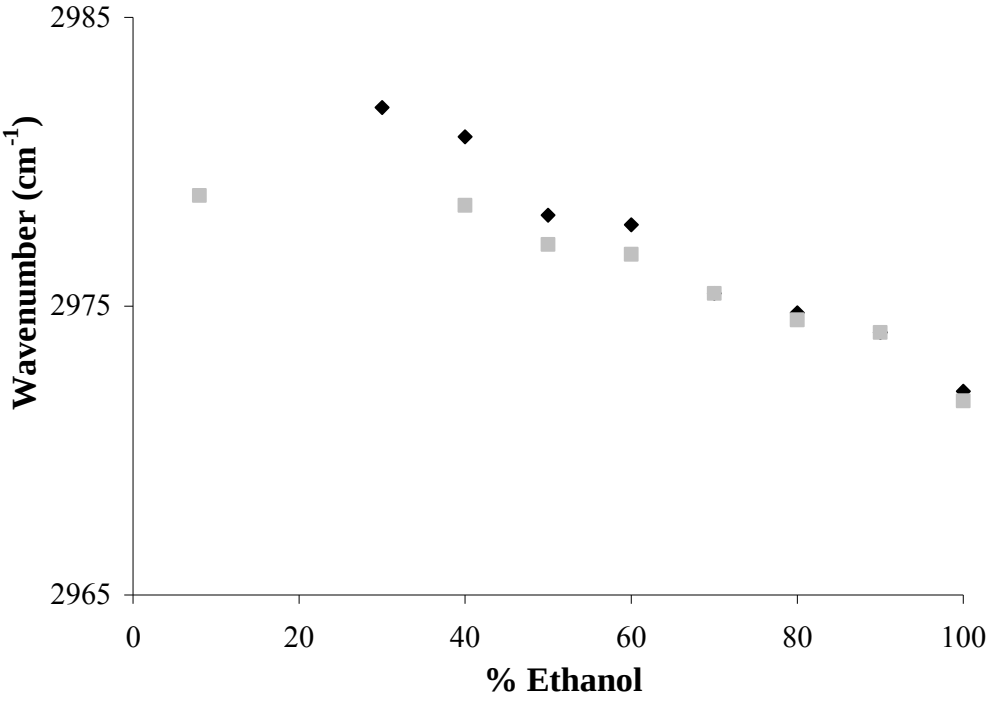
2985
2975
2965
Wavenumber (cm-1)
0
20
40
60
80
100
% Ethanol

c)

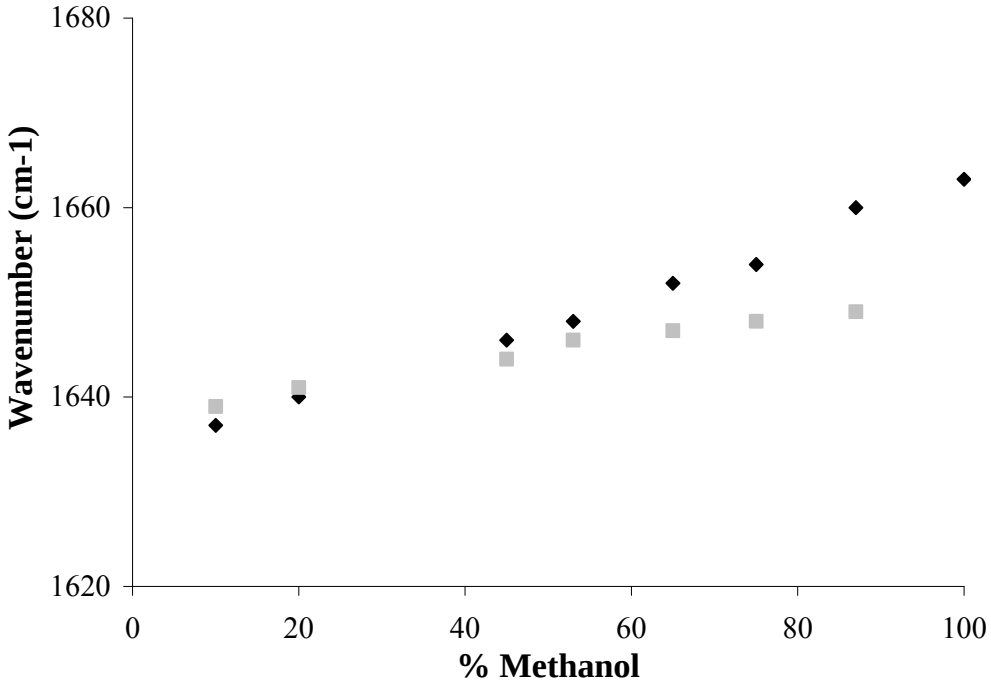
1680
1660
1640
1620
Wavenumber (cm-1)
0
20
40
60
80
100
% Methanol

d)

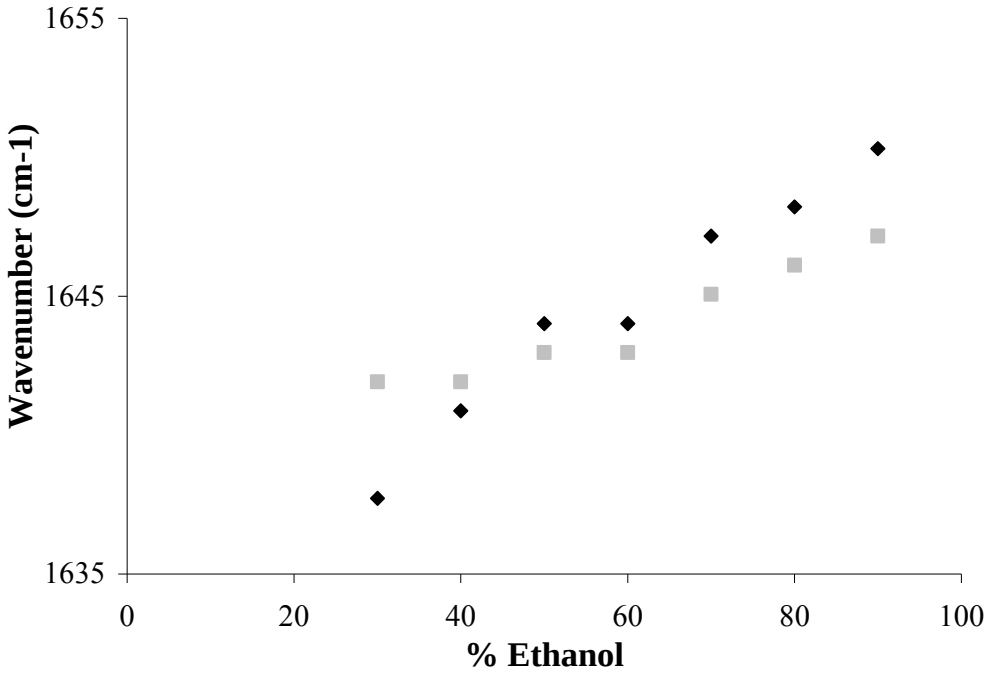

Figure 4.7: a) Specific peak absorbance frequency in: solution spectra (◆); cellulose acetate spectra (■) for a) methanol; b) ethanol; c) water in methanol solution; d) water in ethanol solution.

At high water concentrations, the influence of the hydroxyl peak is stronger [19, 20]. The higher level of hydrogen bonding creates a broader peak and shifts this peak to lower frequency values, thus influencing the peaks of CH_2 and CH_3 vibrations (ethanol and methanol respectively) by peak overlapping effects [21]. Also, the vibrations of the CH_2 and CH_3 groups in the alcohol molecules might be affected by hydrogen bonding of the hydroxyl group present in the molecule. The relation between the alcohol concentration in solution and the absorbance frequency is also almost linear (Figures 4.7c and 4.7d). In the case of the water peak (peak C), the peak maximum shifts to lower frequency values with an increase in water concentration. In principle this would offer the possibility to use this trend to determine solute concentrations based on the frequency shift of specific groups.

4.4.5 Sorption

Typical spectra are given for 50% water/alcohol mixtures and for the CA membrane in contact with these mixtures (Figure 4.8).

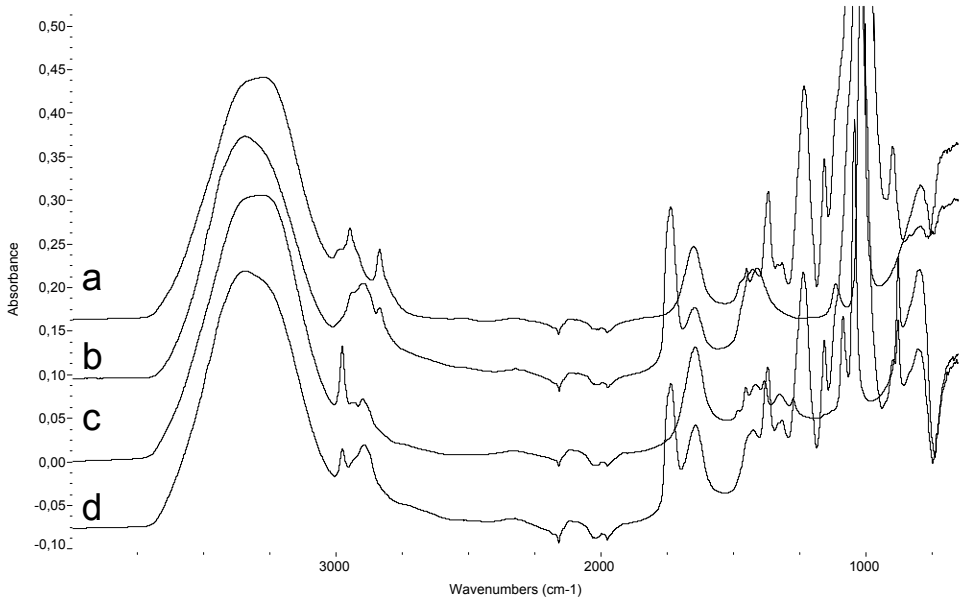

Figure 4.8: Spectra of a) water/methanol solution 50%; b) CA + water/methanol solution 50%; c) water/ethanol solution 50%; d) CA + water/ethanol solution 50%.

Figure 4.9 shows that the area of peak A and B in the respective membrane spectra increases upon an increase in the methanol and ethanol concentration in the solution in contact with the membrane. Since the penetration depth is the same for every experiment, this indicates that the number of methanol and ethanol specific groups in the same membrane volume scanned increases (61% area increase for a 53% increase in solution concentration). Also, the water peak decreases with the decrease of water concentration in solution in the two experiments (area decrease of 68% for a decrease in concentration of 66%).

Comparing the variability calculated with the results obtained for the water/methanol and water/ethanol experiments, we conclude that the gradual increase found in water peak area during these experiments can be related to a change in water absorbed in the membrane matrix and is not

due to the influence of structural differences. However, quantification of sorption is only possible at a known degree of swelling.

a)

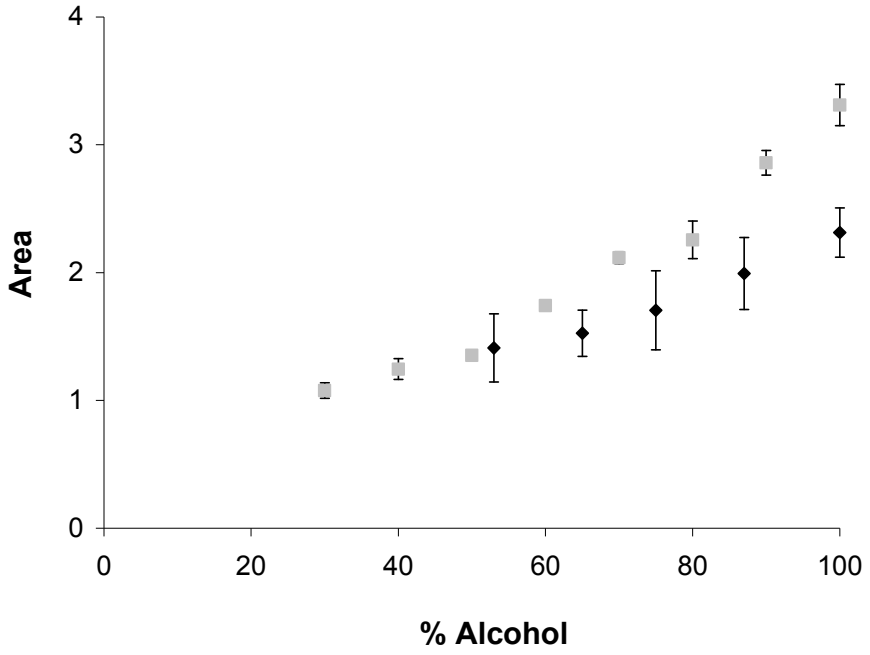

b)

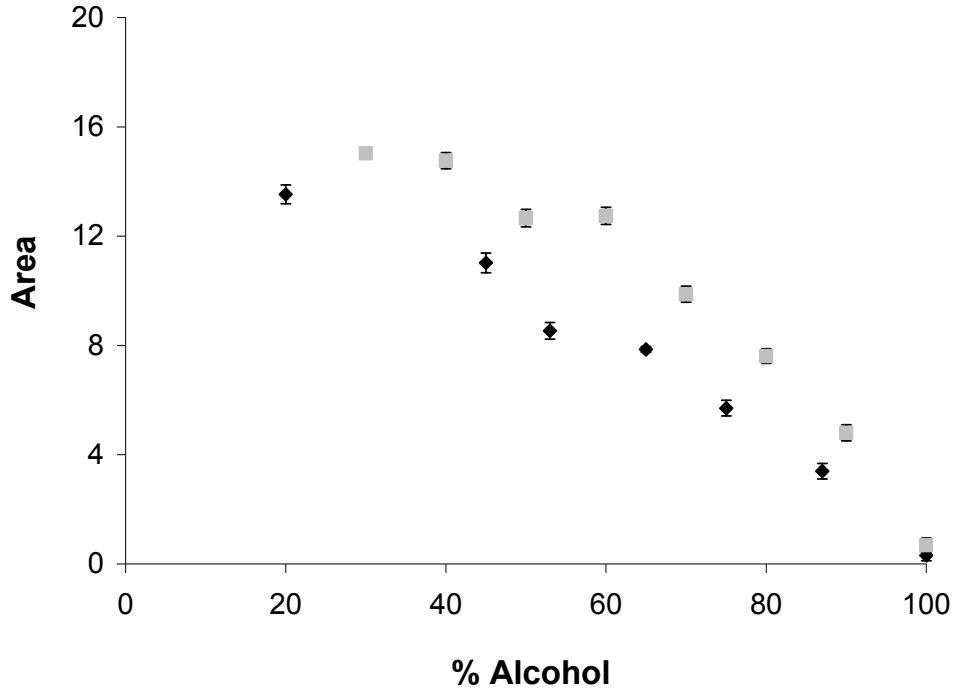

Figure 4.9: Cellulose acetate spectra after 1 hour contact with alcohol solutions: a) gradual change of specific peak area of methanol (◆) and ethanol (■); b) gradual change of water specific peak area in a methanol solution (◆) and in ethanol solution (■).

4.4.6 Preferential sorption

For many applications the sorption selectivity is an important parameter. The values for the selectivity parameter of the membrane for water/methanol or water/ethanol mixtures are plotted in Figure 4.10. In the presence of methanol, the selectivity for water ranges from 2.5 at 52% of methanol in solution to 3.5 at 90%. For water/ethanol mixtures, the selectivity for water ranges from 1 at 30% ethanol to 2 at 90% ethanol. This implies that the membrane preferentially absorbs water. These results are in accordance to the preferential permeation of water found in pervaporation using CA membranes [22-24]. In these papers it is stated that preferential sorption plays a role in the results of the pervaporation experiments. The sorption is greater for water as compared to lower alcohols due to polarity, the effect of hydrogen bonding and the volume available for accommodation in the polymer structure.

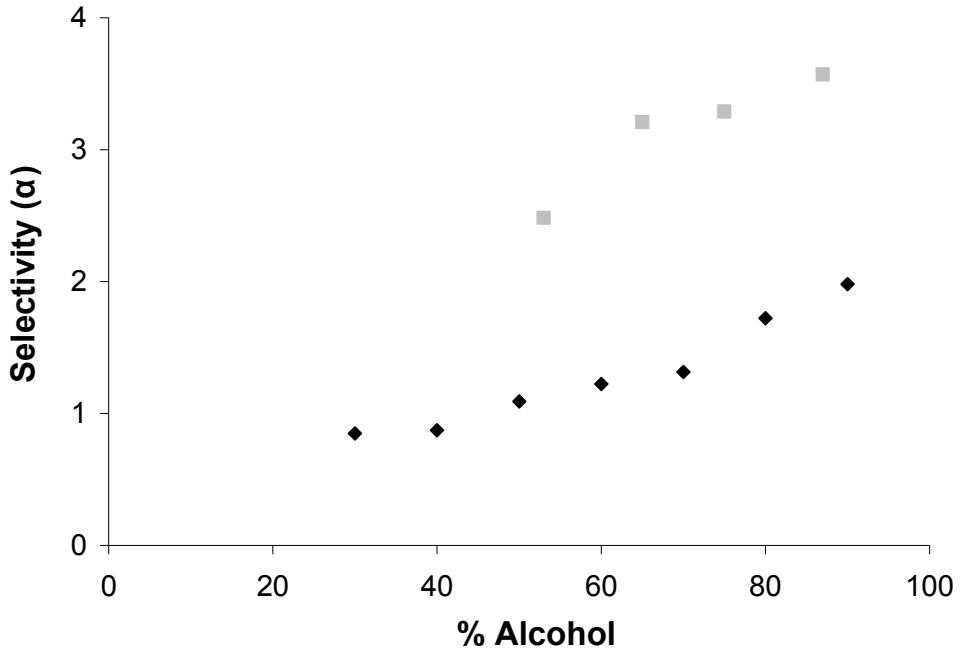

Figure 4.10: Selectivity (α) of CA membrane at various alcohol concentrations in water: (■) methanol; (◆) ethanol.

4.5 Conclusions

ATR-IR allows a non-destructive and easy analysis of the active layer of polymeric membranes. It is possible to determine the dependence of specific peak areas on the concentration of various compounds, both in solution and in the membrane. Preferential sorption of water has been measured in the CA membrane for water/methanol and water/ethanol mixtures, results that are in accordance with literature. From this work we conclude that ATR-IR spectroscopy is likely to become an important tool to study the stability of polymeric membranes in solvent and mixed solvent media solvents.

Acknowledgements

The author would like to thank Bruce Anderson, Peter Thune and Eero Kontturi for their advice on ATR-IR spectroscopy. This project is made within the framework of a Marie Curie Industry Host Fellowship (Contract HPMI-CT-2002-00181).

References

[1] http://www.esig.info, (2004).

[2] M. Timmer, Properties of nanofiltration membranes; model development and industrial application, PhD thesis Technische Universiteit Eindhoven, (2001), ISBN 90-386-2872-2

[3] M. Jacobs, Measurement and modeling of thermodynamic properties for the processing of polymers in supercritical fluids, PhD thesis Technische Universiteit Eindhoven, (2004), ISBN 90-386-2596-0

[4] M. Sanopoulou, J. H. Petropoulos, Sorption and longitudinal swelling kinetic behavior in the system cellulose acetate-methanol, Polymer 38 (1997) 5761-5768

[5] N. H. Brantley, D. Bush, S. G. Kazarian, C.A.Eckert, Spectroscopic Measurement of Solute and Cosolvent Partitioning between Supercritical CO2 and Polymers, J. Phys. Chem. B. 103 (1999) 10007-10016

[6] N. H. Brantley, S. G. Kazarian, C. A. Eckert, In-situ FTIR measurement of carbon dioxide sorption into poly(ethylene terephthalate) at elevated pressures, J. Appl. Polym. Sci. 77 (2000) 764-775

[7] S. G. Kazarian, M. F. Vincent, F. V. Bright, C. L. Liotta, C. A. Eckert, Specific Intermolecular Interaction of Carbon Dioxide with Polymers, J. Am. Chem. Soc. 118 (1996) 1729-1736

[8] S. G. Kazarian, G. G. Martirosyan, Spectroscopy of polymer/drug formulations processed with supercritical fluids: in situ ATR-IR and Raman study of impregnation of ibuprofen into PVP, Int. J. Pharm. 232 (2002) 81-90

[9] S. G. Kazarian, Polymers and supercritical fluids: opportunities for vibrational spectroscopy, Macromol. Symp. 184 (2002) 215-228

[10] C. M. Balik, W. H. Simendinger, III, An attenuated total reflectance cell for analysis of small molecule diffusion in polymer thin films with Fourier-transform infrared spectroscopy, Polymer 39 (1998) 4723-4728

[11] C. Sammon, J. Yarwood, N. Everall, A FTIR-ATR study of liquid diffusion processes in PET films: comparison of water with simple alcohols, Polymer 41 (1999) 2521-2534

[12] M. Ulbricht, G. Belfort, Surface modification of ultrafiltration membranes by low temperature plasma. II. Graft polymerization onto polyacrylonitrile and polysulfone, J. Membr. Sci. 111 (1996) 193-215

[13] V. Freger, J. Gilron, S. Belfer, TFC polyamide membranes modified by grafting of hydrophilic polymers: an FT-IR/AFM/TEM study, J. Membr. Sci. 209 (2002) 283-292

[14] S. Belfer, J. Gilron, O. Kedem, Characterization of commercial RO and UF modified and fouled membranes by means of ATR/FTIR, Desalination 124 (1999) 175-180

[15] S. Belfer, R. Fainchtain, Y. Purinson, O. Kedem, Surface characterization by FTIR-ATR spectroscopy of polyethersulfone membranes-unmodified, modified and protein fouled, J. Membr. Sci. 172 (2000) 113-124

[16] M. W. Urban and Editor, "Attenuated total reflectance spectroscopy of polymers: theory and practice, Am. Chem. Soc. (1996), Washington, DC

[17] A. Idris, A. F. Ismail, M. Noorhayati, S. J. Shilton, Measurement of rheologically induced molecular orientation using attenuated total reflection infrared dichroism in reverse osmosis hollow fiber cellulose acetate membranes and influence on separation performance, J. Membr. Sci. 213 (2003) 45-54

[18] D. Murphy, M. N. de Pinho, An ATR-FT-IR study of water in cellulose acetate membranes prepared by phase inversion, J. Membr. Sci. 106 (1995) 245-257

[19] R. Hester, Handbook of Vibrational Spectroscopy, John Chalmers & Peter Griffiths (eds), Chemistry & Industry, London (2002)

[20] J. Yarwood, C. Sammon, C. Mura, M. Pereira, Vibrational spectroscopic studies of the diffusion and perturbation of water in polymeric membranes, J. Mol. Liq. 80 (1999) 93-115

[21] S. L. Raghavan, B. Kiepfer, A. F. Davis, S. G. Kazarian, J. Hadgraft, Membrane transport of hydrocortisone acetate from supersaturated solutions; the role of polymers, Int. J. Pharm. 221 (2001) 95-105

[22] S. P. Kusumocahyo, T. Kanamori, T. Iwatsubo, K. Sumaru, T. Shinbo, Development of polyion complex membranes based on cellulose acetate modified by oxygen plasma treatment for pervaporation, J. Membr. Sci. 208 (2002) 223-231

[23] S. Mandal and V. G. Pangarkar, Pervaporative separation of a 1-methoxypropanol and water mixture, J. Appl. Polym. Sci. 86 (2002) 2194-2210

[24] K. M. Song, W. H. Hong, Dehydration of ethanol and isopropanol using tubular type cellulose acetate membrane with ceramic support in pervaporation process, J. Membr. Sci. 123 (1997) 27-33

Chapter 5

Dynamic swelling and solvent sorption of a commercial solvent resistant membrane

---

In this chapter the dynamic sorption and swelling behavior of a commercial solvent resistant membrane has been studied for toluene, acetone, n-hexane and five primary alcohols. Swelling has been determined from the increase in sample thickness using two different methods: mechanically with a micrometer and optically with an interferometer. Both techniques show comparable results. For the different alcohols a similar final increase in thickness is observed (6%). Swelling is most pronounced in the case of acetone (9%) and less pronounced in the case of n-hexane and toluene (2%). Different polymer layers present in the membrane show different contributions to swelling: the non-woven support does not swell and the overall thickness increase is mostly governed by the secondary support layer. Modification of the membrane with a silicone-based polymer does not significantly influence the swelling behavior. Comparison of the dynamics of swelling and sorption reveals that these two phenomena, although interdependent, do not start simultaneously and do not reach the same relative value. Furthermore, the extent of sorption is higher for the alcohols as compared to the stronger swelling agent acetone. This implies that interpretation of sorption data in terms of swelling behavior potentially leads to wrong conclusions.

5.1 Introduction

The major application of polymeric membranes has been in aqueous applications. Recently, membranes have also been developed for (nano)filtration of non-aqueous solvents. Complications in the filtration of solvents include the swelling of polymer materials when brought into contact with solvents. In general, swelling has a negative effect on the separation performance as well as on the life-time of a polymer membrane. To minimize the degree of swelling and to tune performance properties, membranes have undergone surface changes and structural modifications [1-3]. Various highly crosslinked membranes have been presented in literature for solvent filtration, specifically developed to withstand the solvent environment and elevated pressure [4-6]. The fast advancements in the development of membranes for non-aqueous solvent filtration will result in an increasing number of possible solvent/membrane combinations. This number is further enlarged by the fact that properties of solvent resistant membranes are not only determined by intrinsic materials properties, but also by details of the fabrication process [7]. As a consequence, fast and simple techniques are required to study the large number of specific solvent/membrane systems.

Various techniques are available to study solvent sorption and swelling of polymers for which an overview has been presented [8]. Many of the techniques used for swelling studies are based on measuring the weight increase of the sample, thereby presuming a direct relation between sorption and swelling [9-12]. Only a few techniques have been presented to directly measure the change in membrane volume [13, 14]. Other potential techniques exist, but have not been applied to study membrane swelling. Examples include optical techniques, such as interferometry. Interferometry is a fast non-contact optical technique that allows measurement of in-situ swelling of a membrane. This technique relies on the interference of light beams that have traveled optical paths of different lengths. A typical interferometer splits light from a single source into a beam that is reflected on a reference mirror and a beam that is reflected on the sample. Both reflected beams are transmitted to a sensor that records the intensity as a function of sample displacement along the optical axis. The recorded intensity shows a maximum when the difference in optical path lengths is zero. When a CCD image sensor is used, simultaneous measurement of a number

of points on the sample surface is possible, from which the 3D surface topology can be reconstructed [15-17].

In this chapter the dynamic swelling behavior of a commercial membrane is studied by measuring the thickness increase in time. Two straightforward techniques are used for this purpose: optically using an interferometer and mechanically using a micrometer. The dynamics of swelling are studied for a number of solvents and the results are compared with the dynamic sorption behavior.

5.2 Experimental

Swelling measurements were performed using Solsep 030206 membranes (Solsep, the Netherlands). These membranes consisted of two distinct layers (see Figure 5.1): a non woven support layer of approximately 150 μm thickness (layer A) and a secondary support layer of approximately 50 μm with a finger-like structure (layer B).

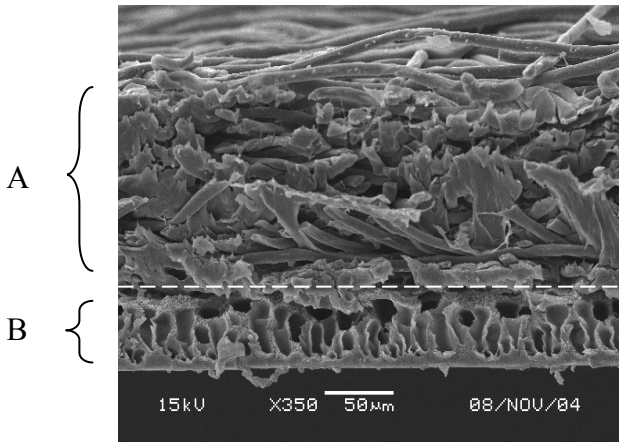

Figure 5.1: SEM image of a Solsep 030206 solvent resistant nanofiltration commercial membrane.

The nanofiltration capabilities of the membrane were obtained by modification using a silicon type polymer. Measurements were performed on samples containing: only the non-woven support (layer A), the non-woven support and the finger-like structure (layer A+B), or the full

nanofiltration membrane. For analysis of each layer, the samples used were taken from the same sheet of membrane. Methanol (99%), ethanol (99%), 1-propanol (99%), 1-butanol (99%), 1-pentanol (99%), acetone (99.9%), toluene (99.9%), n-hexane (99.9%) were obtained from Sigma-Aldrich.

5.2.1 Mechanical thickness measurements

Mechanical thickness measurements were performed using an Absolute Digimatic, 293 series thickness meter (Mitutoyo, Japan) with a range of 0 to 25 mm and an error of 0.5 μm. The contact area of the thickness meter was increased to 9.5×10^{-5} m^2 to ensure that the pressure exerted on the samples remained below 1 bar. For each solvent the measurements were repeated on 5 different samples. First, the initial thickness of every sample was measured prior to contact with the solvent. In short-term experiments the sample thickness was measured after exposing the sample to the solvent up to 15 times. Solvent exposure was done by dipping the sample in the solvent for 10 seconds and subsequently wiping off the excess of solvent. In long-term experiments the samples were constantly kept in contact with the solvent for a period of several days. The thickness of layer B was obtained after subtracting the average thickness of the non-woven support. The relative increase in thickness of an exposed sample was determined with reference to the unexposed sample.

5.2.2 Optical thickness measurements

Interferometry measurements were performed using a Fogale ZoomSurf 3D (Fogale Nanotech, France) equipped with a 20× coaxial interference Mireau objective (Leica Microsystems GmbH, Germany). The data were analyzed using the software Fogale Map (Fogale Nanotech, France). Samples were prepared by taking a 50 μm thick slice from layer B with the help of a scalpel. No material of the non-woven support was present in these samples. To overcome the tendency of the polymer to curl, slices were placed on top of a glass plate using double-sided tape. For each solvent the measurements were repeated on 3 different samples and for each sample the thickness was measured at 6 different locations. The sample was first measured for the initial thickness.

Exposure was done by placing a drop of the solvent on top of the sample. The excess of solvent is removed with the help of absorbing paper. The layer of solvent remaining is then absorbed by the polymer. Thickness was measured and the procedure was repeated up to 10 times.

5.2.3 Sorption measurements

Directly after a mechanical thickness measurement the sample was placed in a closed vial and its weight was determined using a Sartorius BP 221s balance (Sartorius Technologies, the Netherlands), with an accuracy of 0.05 mg. The typical weight of a dry sample is approximately 20 mg.

5.3 Result and discussion

5.3.1 Short term swelling behavior

5.3.1.1 Mechanical thickness determination

In Figure 5.2 the short term swelling behavior mechanically determined for the nanofiltration membrane is presented for methanol, ethanol and 1-propanol.

The results show that the short term swelling behavior is strongly influenced by the nature of the applied solvent. For methanol, already after one single exposure an increase in thickness of 2.6% is observed. The increase in thickness remains more or less constant for the subsequent 10 exposures. The following measurements show that swelling has not reached a steady state point and the membrane continues to increase in thickness. In contrast, for ethanol the extent of swelling after a single exposure is only 0.4%, but after 4 exposures the increase in thickness is similar to that observed for methanol (2.3%). As well as for methanol, upon additional exposure to ethanol, the membrane shows further increase in thickness. For 1-propanol swelling only starts after the sample has been exposed to the solvent 10 times. After 15 exposures the swelling becomes comparable to that observed for methanol and ethanol. For 1-butanol, 1-pentanol, toluene and n-hexane no swelling is observed within the timeframe of the short-term experiments.

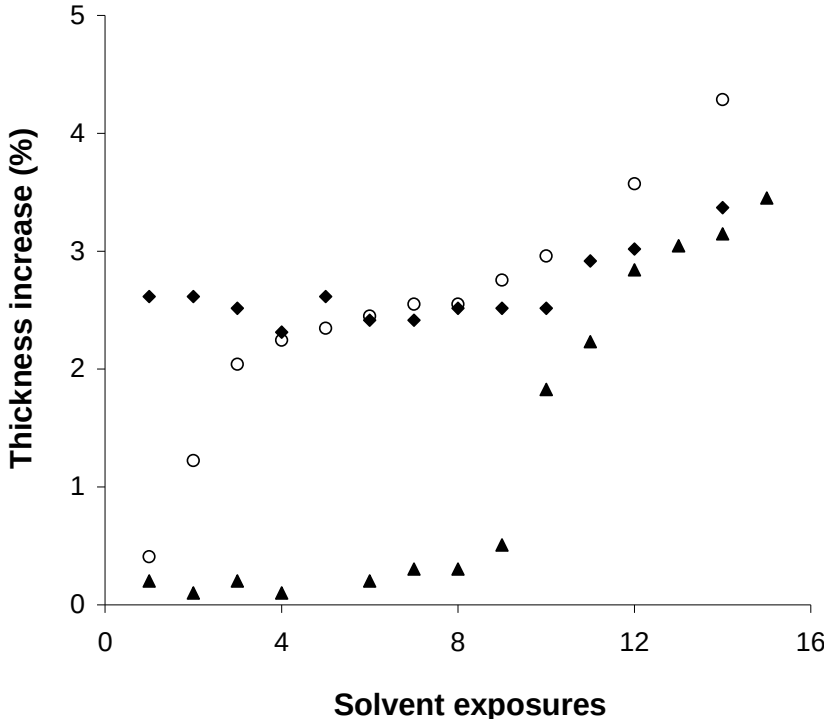

Figure 5.2: Thickness increase (%) of a modified Solsep 030206 when exposed to (◆) methanol, (O) ethanol and (▲) 1-propanol.

Figure 5.3 shows the swelling of the individual layers present in the membrane. For each layer the increase in thickness has been normalized with respect to the initial layer thickness prior to solvent exposure. Clearly, the support layer A shows no significant swelling for methanol and ethanol. A similar behavior is found for all other solvents used in this study, also in the long term experiments discussed further on in this chapter. The same results have been found in literature for the same type of support material [13]. The overall swelling is governed by layer B. In the case of ethanol the extent of swelling of layer B shows an increase with the number of exposures. The swelling behavior appears to be unaffected by the modification with the silicon based polymer. For methanol, initially, a smaller increase in thickness is observed for the samples that have been modified with the silicon polymer as compared to the unmodified samples. The difference is much less pronounced after 12 exposures, as will also become evident in the long term experiments. The origin of this difference is unclear.

a)

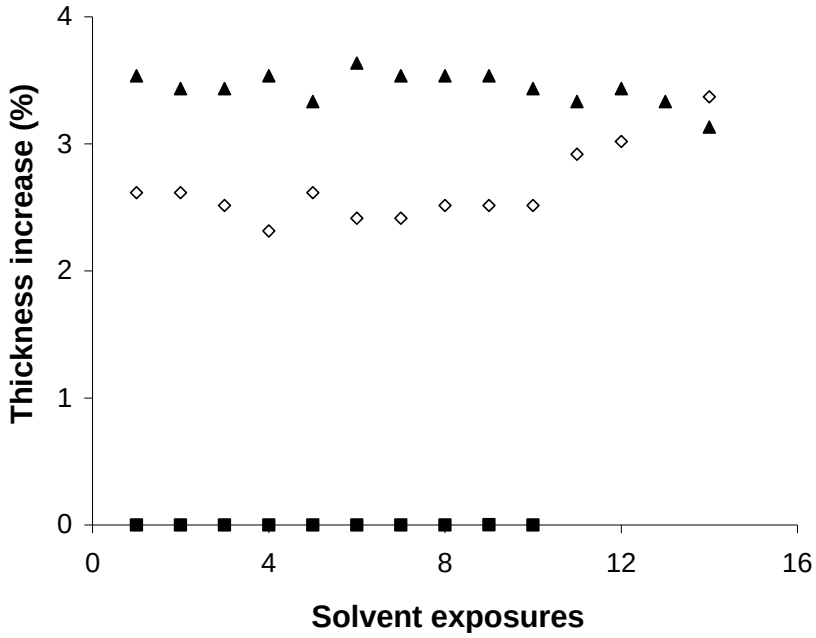

b)

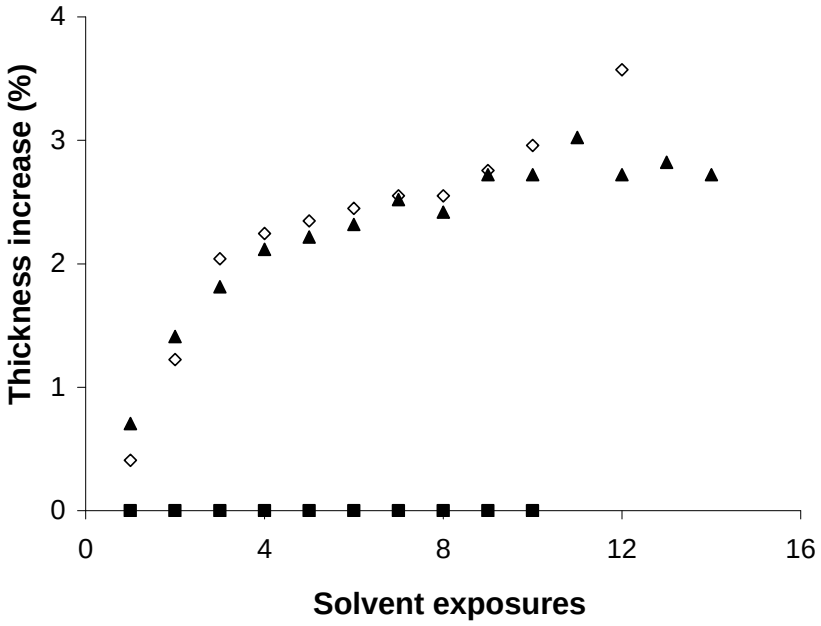

Figure 5.3: Thickness increase (%) of the individual membrane layers: (■) layer A; (▲) layer B and (◊) modified Solsep 030206 when exposed to a) methanol and b) ethanol.

5.3.1.2 Optical versus mechanical thickness measurements

Figure 5.4 shows the short term swelling behavior of layer B modified with the silicon based polymer, determined with both the optical and mechanical method. The two methods yield similar results for methanol; the thickness increases rapidly to a more or less constant value of 10-12%. For ethanol both methods yield a similar trend, however, the increase in thickness after a single exposure is already much higher in the case of the optical method. This may be related to the difference in the method of solvent exposure used for the two techniques; a higher degree of swelling per exposure will shift the data to the left. For the final two ethanol exposures the optical method probably overestimates the swelling due to delamination of the sample from the double sided tape. Delamination became a problem also for the case of 1-propanol. 1-Propanol dissolved the glue present in the double sided tape causing immediate separation of the sample and the glass plate.

a)

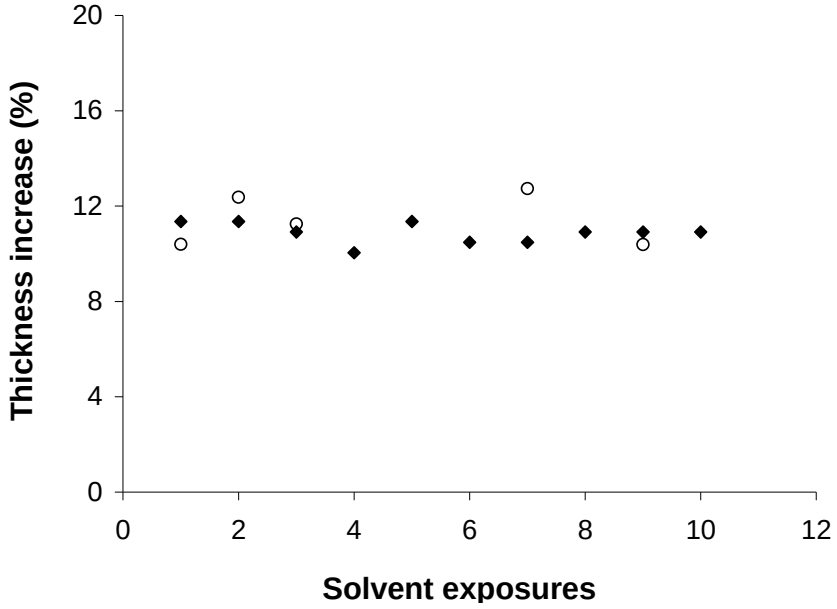

b)

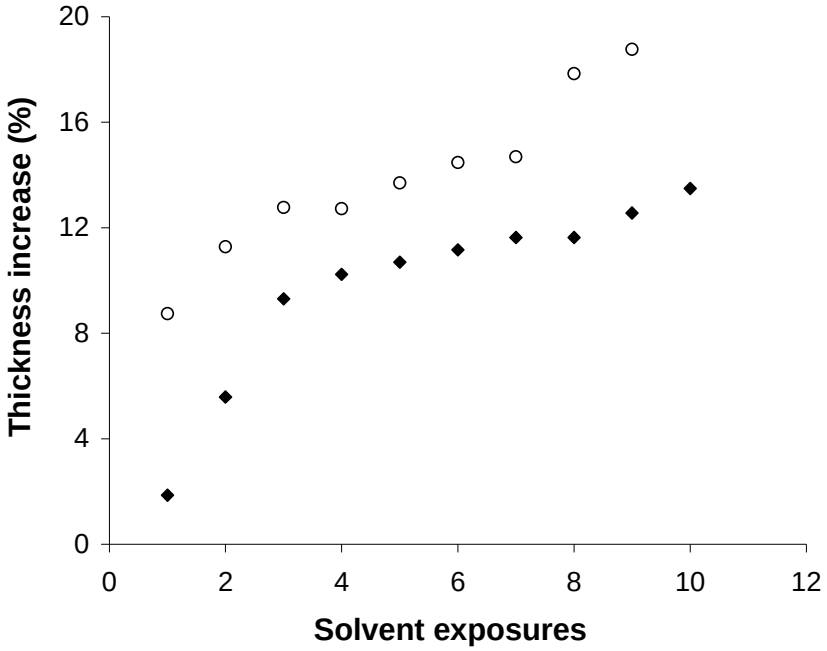

Figure 5.4: Thickness increase (%) of the modified Solsep 030206 when exposed to a) methanol and b) ethanol using: (◆) mechanical technique and (O) optical technique.

The results indicate that interferometry is applicable for dynamic swelling studies, but has drawbacks, including restrictions with respect to sample preparation and the fact that it can not be applied under realistic nanofiltration conditions. Under such conditions swelling will be influenced by compaction, resulting from the applied pressure. The mechanical method does allow simulation of the static pressure, simply by changing the applied pressure.

5.3.2 Long term swelling behavior

Figures 5.5 a-h show the long term swelling behavior for the different solvents used in this study. Data are presented for silicon polymer modified membranes as well as unmodified membranes. The increase in thickness is normalized with respect to the thickness of the sample prior to exposure.

a)

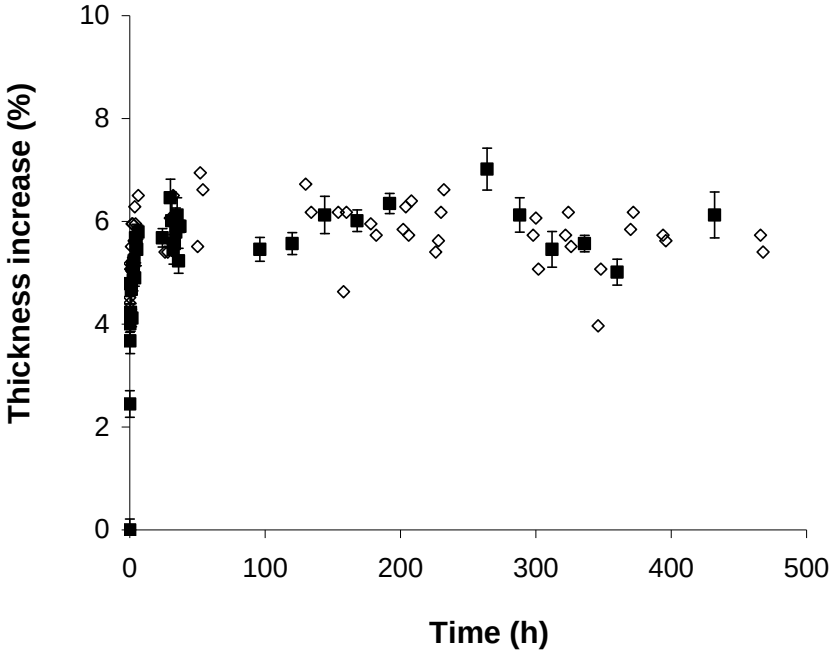
Thickness increase (%)
Time (h)
0
2
4
6
8
10
0
100
200
300
400
500

b)

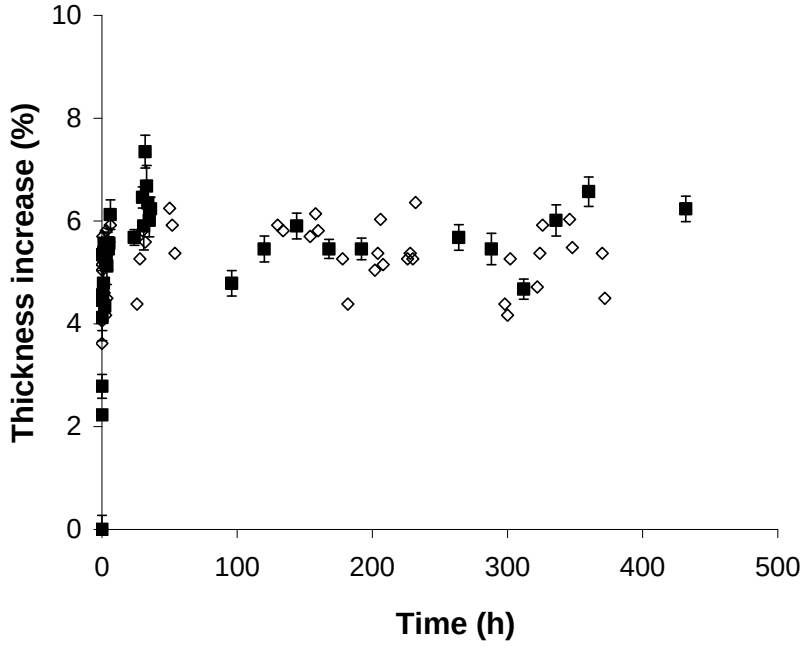
Thickness increase (%)
Time (h)
0
2
4
6
8
10
0
100
200
300
400
500

c)

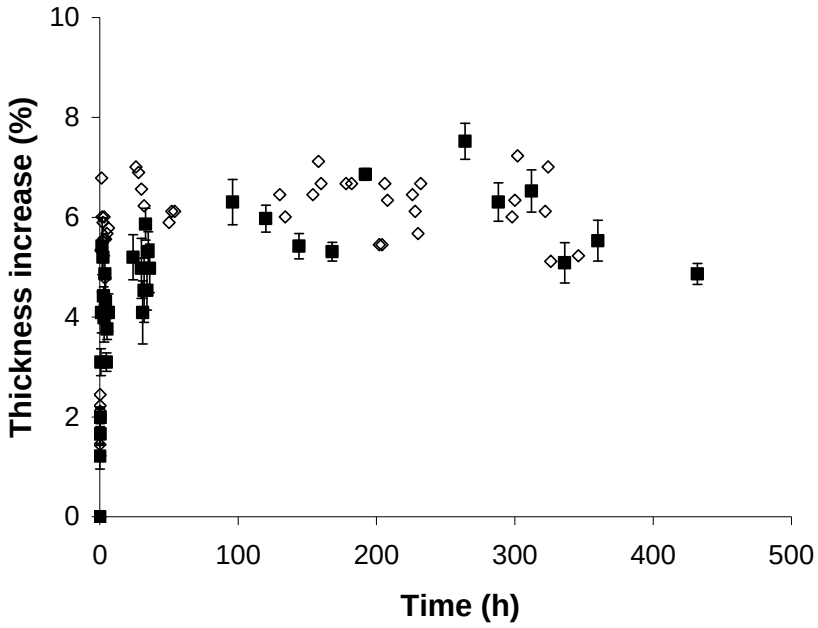
Thickness increase (%)
0
2
4
6
8
10
0
100
200
300
400
500
Time (h)

d)

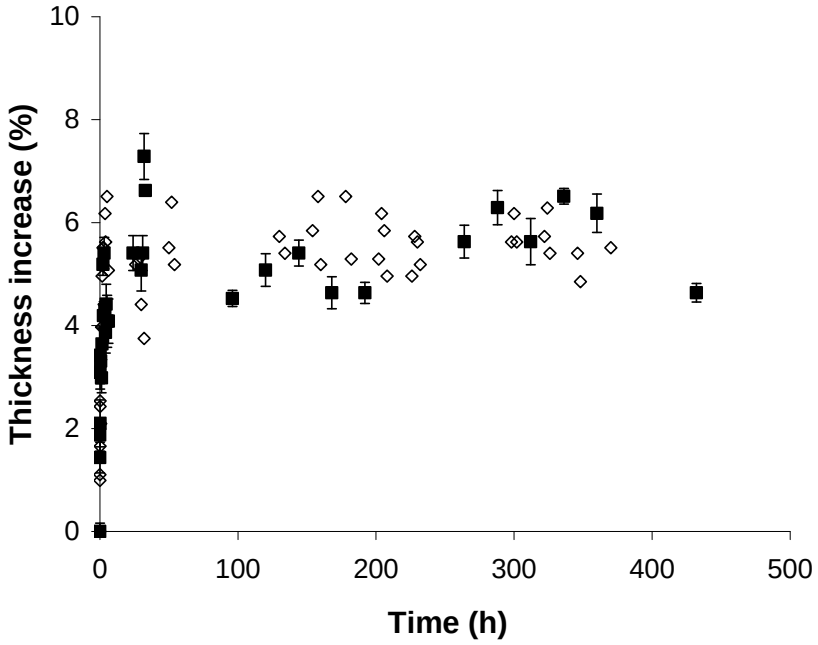
Thickness increase (%)
0
2
4
6
8
10
0
100
200
300
400
500
Time (h)

e)

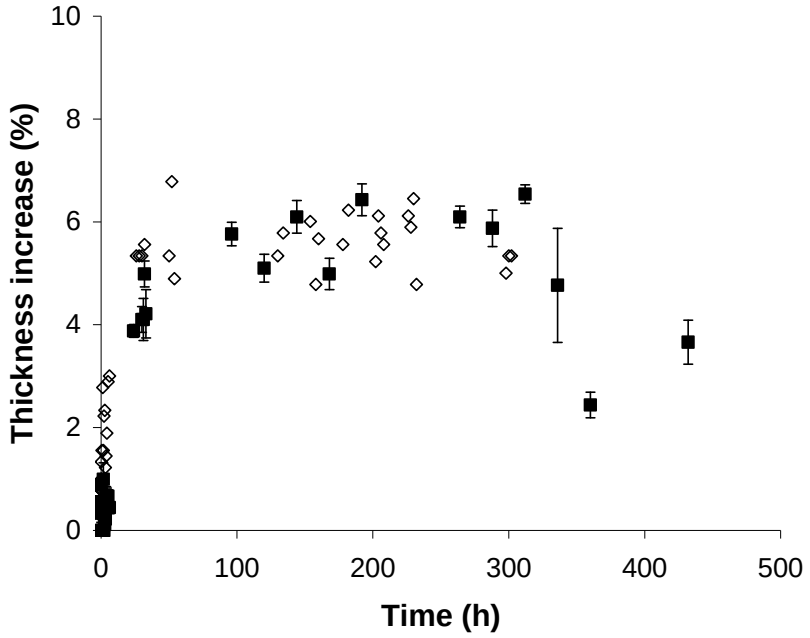
Thickness increase (%)
Time (h)
0
2
4
6
8
10
0
100
200
300
400
500

f)

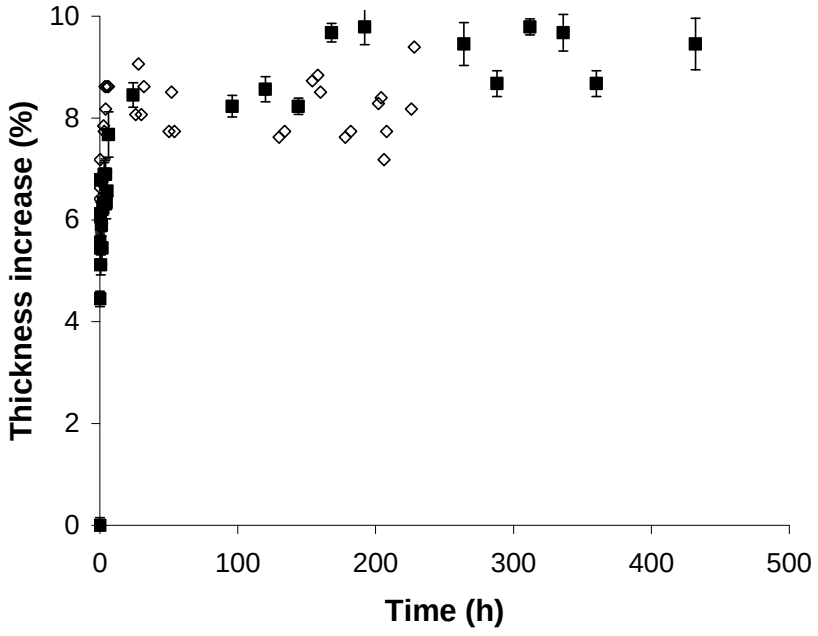
Thickness increase (%)
Time (h)
0
2
4
6
8
10
0
100
200
300
400
500

g)

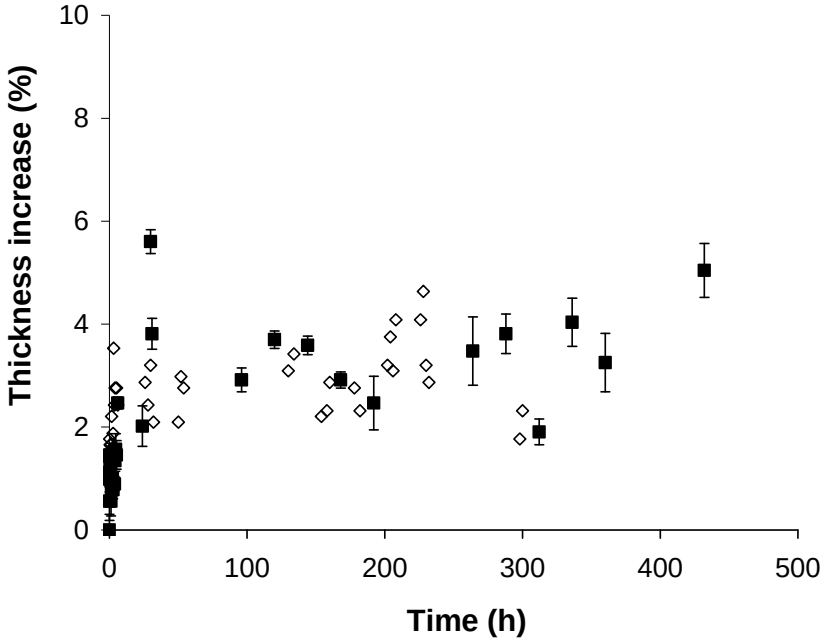

h)

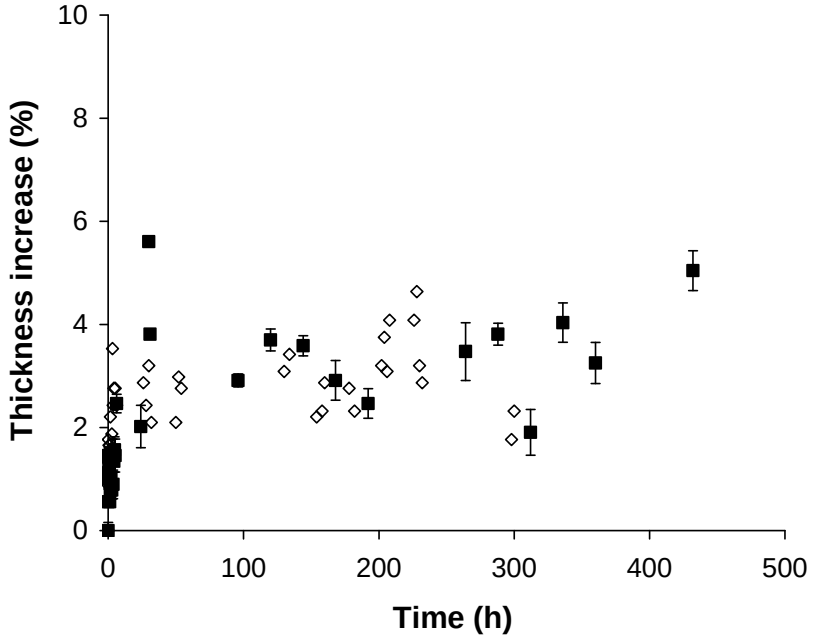

Figure 5.5: Thickness increase (%) of (■)modified Solsep 030206 and (◊) unmodified Solsep 030206 when exposed to: a) methanol; b) ethanol; c) 1-propanol; d) 1-butanol; e) 1-pentanol; f) acetone; g) toluene h) n-hexane. The error shown relates to the standard error of the measurement.

For all solvents the modification has no significant influence on the final degree of swelling. The largest increase in sample thickness is observed for acetone, approximately 9%. The smallest increase in thickness is observed for n-hexane and toluene, approximately 2%. For the different alcohols a similar degree of long term swelling is observed, approximately 5-7%. Although the initial rate of swelling varies for the different solvents, after 10 hours a steady state value is observed in all cases except for 1-pentanol. For 1-pentanol swelling evolves slower. These results suggest that pre-swelling procedures should be considered prior to any non-aqueous membrane application.

5.3.3 Swelling versus sorption

Figure 5.6 shows the simultaneous dynamic sorption and swelling behavior in time in the case of methanol (a), acetone (b) and 1-pentanol (c).

a)

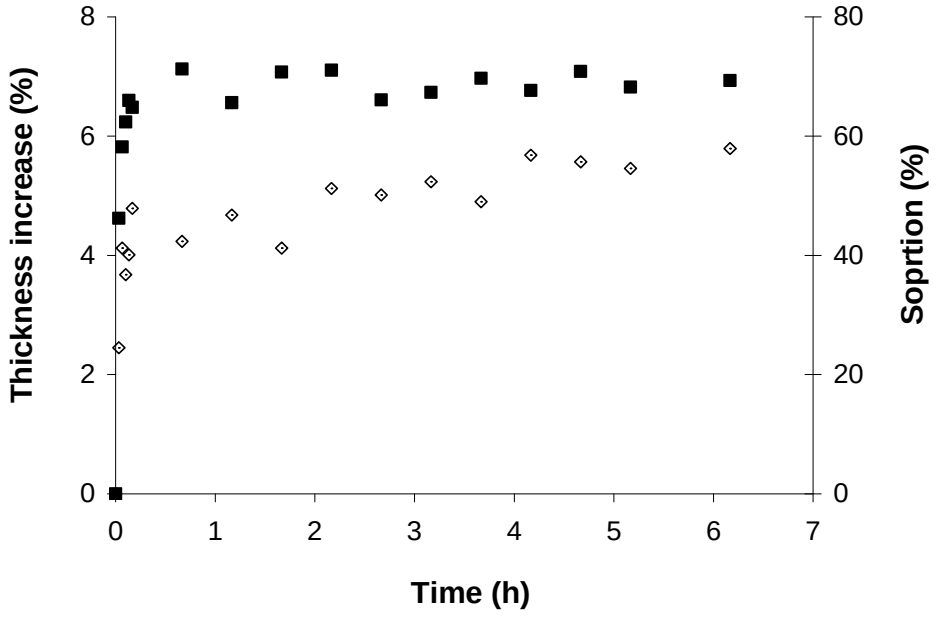

b)

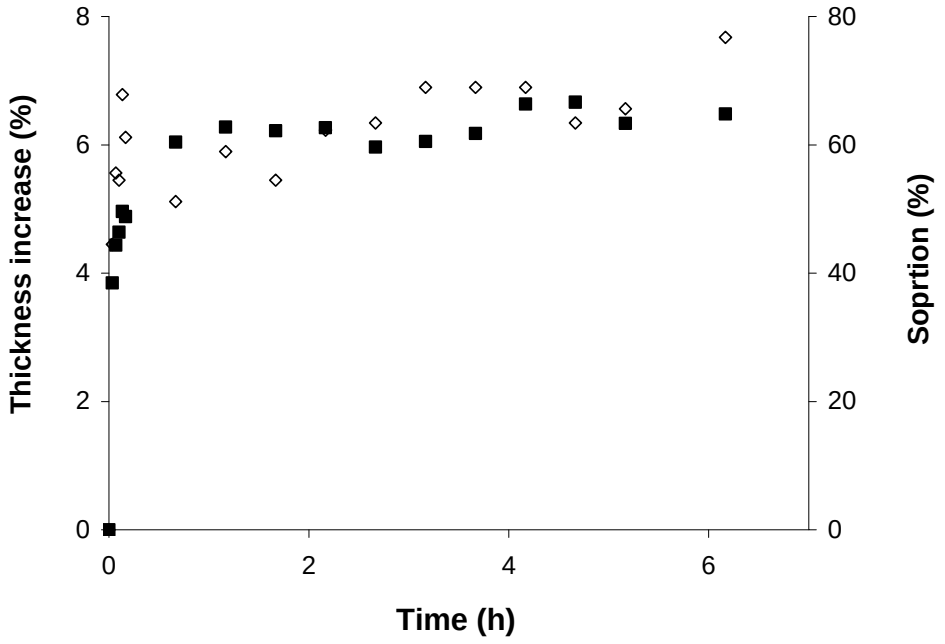

c)

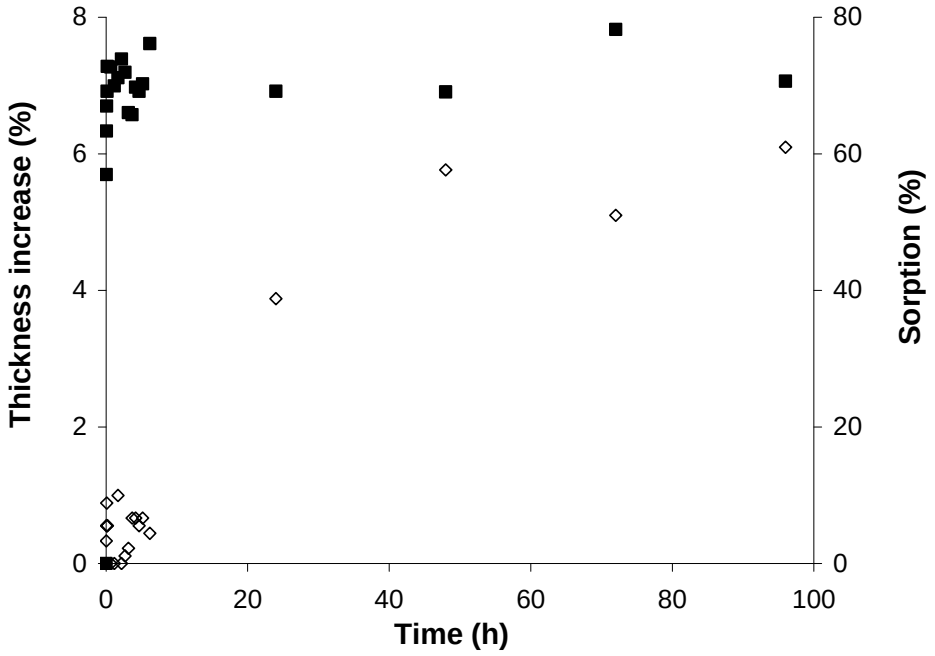

Figure 5.6: (◊) Thickness increase (%) and (■) sorption of Solsep 030206 for a) first 7 hours of contact with methanol; b) first 7 hours of contact with acetone and c) 100 hours of contact with 1-pentanol.

In the case of methanol and acetone, both swelling and sorption start instantly upon contact between the sample and the solvent. Sorption equilibrium is reached while the thickness of the membrane is still increasing. 1-Pentanol swelling shows initially a delay, followed by a very slow thickness increase. The final degree of swelling is observed only after 40 hours of contact. A similar contrast between swelling and sorption behavior has been found for 1-propanol, 1-butanol, toluene and n-hexane. For methanol and 1-pentanol the final increase in thickness is 6% and the corresponding increase in weight is 70%. In contrast, in the case of a strong swelling agent like acetone, a larger increase in thickness is observed (9%) while the weight increase is smaller (60%). This implies that interpretation of sorption data in terms of swelling behavior can potentially lead to wrong conclusions.

5.4 Conclusions

Two straightforward techniques have been used to measure swelling: mechanically using a micrometer and optically using an interferometer. Both methods allow study of the dynamic swelling behavior and yield similar results. However, the optical method has restrictions on sample preparation and can not be applied under pressurized conditions. The results obtained from the two distinct methods correspond well and show that even for rather similar molecules, such as a homologous series of primary alcohols, different swelling behavior can occur. Furthermore, different polymer layers present in the membrane show different contributions to swelling: the non-woven support of the membrane does not swell significantly and the overall thickness increase is mostly governed by the secondary support layer with fingerlike structure. Modification of the membrane with a silicon-based polymer does not significantly influence its swelling behavior.

Comparison of the dynamics of swelling and sorption reveals that these two phenomena, although interdependent, do not start simultaneously and do not reach the same relative value. Furthermore, results show that if the extent of sorption is interpreted as a direct measure for the extent of swelling, incorrect conclusions can be drawn. This suggests that a simple measurement

of thickness using a micrometer provides more accurate information on swelling than complicated weight-based methods.

References

[1] S. Aerts, A. Vanhulsel, A. Buekenhoudt, H. Weyten, S. Kuypers, H. Chen, M. Bryjak, L. E. M. Gevers, I. F. J. Vankelecom, P.A. Jacobs, Plasma treated PDMS-membranes in solvent resistant nanofiltration: Characterization and study of transport mechanism, J. Membr. Sci. 275 (2005) 212-219

[2] L. E. M. Gevers, I. F. J. Vankelekom, P. A. Jacobs, Zeolite filled PDMS as an improved membrane for solvent resistant nanofiltration (SRNF), Chem. Commun. (2005) 2500-2502

[3] L. E. M. Gevers, I. F. J. Vankelecom, P. A. Jacobs, Solvent resistant nanofiltration with filled PDMS membranes, J. Membr. Sci. 278 (2006) 199-204

[4] D. A. Musale, A. Kumar, Solvent and pH resistance of surface crosslinked chitosan/PAN composite nanofiltration membranes, J. Appl. Polym. Sci. 77 (1999) 1782-1793

[5] J. Jegal, K. Lee, Nanofiltration membranes based on poly(vinyl alcohol) and ionic polymers. J. Appl. Polym. Sci. 72 (1998) 1755-1762

[6] E. S. Tarleton, J. P. Robinson, C. R. Millington, A. Nijmeijer, M. L. Taylor, The influence of polarity on flux and rejection behavior in solvent resistant nanofiltration – experimental observations J. Membr. Sci. 278 (2006) 318-327

[7] E. S. Tarleton, J. P. Robinson, M. Salman, Solvent-induced swelling of membranes – measurements and influence in nanofiltration, J. Memb. Sci. 208 (2006) 442-451

[8] M. Jacobs, Measurement and modelling of thermodynamic properties for the processing of polymers in supercritical fluids, PhD thesis, Technische Universiteit Eindhoven (2004), ISBN 90-386-2596-0

[9] J. Geens, B. van der Bruggen, C. Vandecasteele, Characterization of the solvent stability of polymeric nanofiltration membranes by measurement of contact angles and swelling, Chem. Eng. Sci. 59 (2004) 1161-1164

[10] B. Shi, C. Feng, Y. Wu, A new method of measuring alcohol clusters in polyamide membrane: combination of inverse gas chromatography with equilibrium swelling, J. Membr. Sci. 245 (2004) 87-93

[11] B. Shi, B. Gao, Z. Wang, Y. Wu, Accounting for the degree of swelling in polyimides with a free volume distribution theory, J. Membr. Sci. 264 (2005) 122-128

[12] I. Vankelecom, K. Smet, L. Gevers, A. Livingston, D. Nair, S. Aerts, S. Kuypers, P. Jacobs, Physico-chemical interpretation of the SRNF transport mechanism for solvents through dense silicone membranes, J. Membr. Sci. 231 (2004) 99-108

[13] E. Piccinini, M. Giacinti Baschetti, G. C. Sarti, Use of an automated spring balance for the simultaneous measurements of sorption and swelling in polymeric films, J. Membr. Sci. 234 (2004) 95-100

[14] E. S. Tarleton, J. P. Robinson, S. J. Smith, J. J. W. Na, New experimental measurements of solvent induced swelling in nanofiltration membranes, J. Membr. Sci. 261 (2005) 129-135

[15] K. Creath, Phase measurement interferometry techniques, Progress in Optics, vol. XXVI (1998) 349-393 Editions North Holland Publishing Company, Netherlands

[16] S. Diddams, J. C. Diels, Dispersion measurements with white-light interferometry, J. Opt. Soc. Am. B13 (1996) 1120-1129

[17] S. Petitgrand, R. Yahiaoui, K. Danaie, A. Bosseboeuf, J.P. Gilles, 3D measurement of micromechanical devices vibration mode shapes with a stroboscopic interferometric microscope, Opt. Laser. Eng. 36 (2001) 77–101

Chapter 6

ATR-IR method for in-situ study of compaction in asymmetric nanofiltration membranes

---

Attenuated total reflectance infrared spectroscopy (ATR-IR) is used for in-situ study of compaction of the active layer of a commercial solvent resistant nanofiltration membrane. The amount of energy absorbed during the ATR-IR measurements is related to the sample density and increases with applied pressure. The pressure-induced compaction is partly irreversible. An increase in pressure of 40 bar results in a density increase of 20%. With a subsequent reduction in pressure down to 10 bar 13% of the density increase remains. Compaction in the active layer is not directly related to the total thickness of the membrane. For an increase in pressure of 40 bar the membrane thickness will decrease 6%. A subsequent reduction in pressure shows a further decrease in thickness, reaching 20% at 10 bar. A similar hysteresis effect is observed for the transport of methanol, where a continuous reduction in permeance is observed for an increase and subsequent decrease in transmembrane pressure. The influence of compaction on the transport of 1-butanol is insignificant. This minor effect is attributed to the predominantly diffusive transport of 1-butanol. The reduction of free volume has a more significant influence on viscous transport, which is predominant for methanol.

6.1 Introduction

Nanofiltration is a process driven by transmembrane pressures up to 50 bar. The commercial nanofiltration membranes available nowadays are made of different polymer layers that are susceptible to compaction in this pressure range. Compaction is the decrease in membrane volume due to mechanical deformation upon the application of a high mechanical pressure. Furthermore, compaction will counteract swelling, i.e compaction is expected to reduce the extent of swelling. A change in density of the active layer of the membrane implies a change in free volume available. This will have a significant influence on transport of permeating components. In literature, quantification studies of membrane compaction are limited and the phenomenon is usually related to a change in permeability [1-5]. Ebert et. al. [6] presented a study of the influence of compaction to the pore distribution, where a reduction in porosity of 83% was found for an applied pressure of 30 bar. Peterson et. al. [7] and Reinsch et. al. [8] presented experiments where compaction of an asymmetric membrane was measured in-situ during permeation experiments, using ultrasonic time-domain reflectometry (UTDR). In their method the change in the total thickness of the membrane is determined from a time-of-flight analysis. This approach is inherently susceptible to surface morphology and mechanical changes other than compaction, e.g. bending. Furthermore, the change in thickness of the membrane is not necessarily representative for the compaction of the active layer, especially when the membrane comprises layers of different materials. Vankelecom et. al. [9] studied swelling and compaction effects in samples consisting only of a single material, corresponding to that present in an active layer. The limitation of such a method is related to the complex structure of many commercial membranes used in solvent application. In a number of these membranes the active layer is a result of a surface modification of an existing porous layer. For this reason, the properties of such active layers are not comparable to the properties of the original polymers. Consequently, a technique that allows direct measurement of compaction of the active layer is very important. Attenuated total reflectance infrared spectroscopy (ATR-IR) is a technique developed for characterization of solid samples. This technique, already discussed in Chapter 4, is extremely versatile and allows measurement of many physical and chemical phenomena such as sorption,

swelling and compaction. Measurements can also be performed with a sample under gas or liquid conditions. Direct quantification based on ATR-IR measurements is not straightforward [10], however, changes in the spectra can lead to conclusive results [11, 12]. Kazarian and co-workers have focused strongly on techniques such as ATR-IR, in some cases coupled to imaging techniques, to characterize polymer structures in different applications. Some examples have been shown in Chapter 4. Recently, measurements on moisture and compression effects on the density of pharmaceutical tablets using ATR-IR imaging have been discussed [13-15]. In these studies the basic concept relies on the change in density of the sample under pressure. Density will influence the amount of energy absorbed from the infrared beam and consequently the resulting spectrum will change. This approach opens a window of opportunity to develop in-situ membrane compaction measurements, restricting the measurement to the active layer.

This work will show the applicability of ATR-IR for studying compaction behavior of a commercial solvent resistant membrane (Solsep 030206). The method allows measurement of compaction of only the active layer, at different pressure conditions.

6.2 Method

Figure 6.1 is a schematic representation of a membrane compaction measurement using ATR-IR.

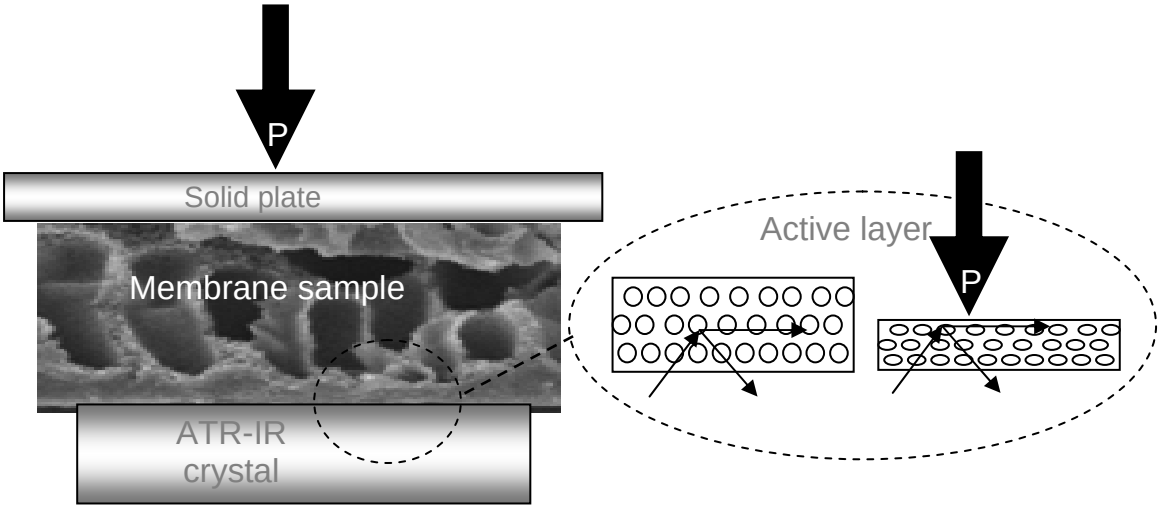

Figure 6.1: Schematic representation of experimental set-up.

A membrane sample is placed with the active layer contacting the ATR-IR diamond crystal. The penetration depth of the light beam is in the order of 1 μm, which is usually smaller than the thickness of the active layer. Consequently, the ATR-IR measurement will only give information on changes of this active layer. When pressure is applied to the sample, by exerting a controlled force on a solid plate placed on top of the membrane, the volume of the active layer will decrease. This is depicted on the right side of Figure 6.1. The result is an increase in density of functional groups, represented by circular symbols (O). This will in turn result in an increase in the amount of energy absorbed from the light beam by the sample [13].

6.3 Experimental

A commercial membrane was used (Solsep 030206, Solsep B.V., the Netherlands). ATR-IR spectra were recorded with a 8400S Fourier transform infrared spectrophotometer (FTIR) from Shimadzu, using a Nicolet Smart Golden gate Mk II total reflectance device with a diamond crystal at an incidence angle of 45°. Each spectrum resulted from 32 scans at 4 cm^{-1} resolution for a spectral range from 4000 to 400 cm^{-1}. All the readings were performed at room temperature and were within a confidence interval of 95% based on 10 measurements. Pressure was applied by a force-calibrated screwdriver from Specac Ltd, UK. The pressure was varied in the range of 10 to 100 bar and for a period of 1 minute.

Thickness experiments were performed using an Absolute Digimatic, 293 series thickness meter (Mitutoyo, Japan) with a range of 0 to 25 mm and an error of 0.5 μm. The area of the micrometer in contact with the sample was increased to ensure that the pressure exerted on the samples remained below 1 bar. Compaction was induced by applying a pressure in the range of 10-100 bar to the samples for one minute. After this, the pressure was relieved and the sample thickness was measured. For all samples, hysteresis type experiments were performed, with pressure steps of 10 bar.

6.4 Results and discussion

Figure 6.2 shows two typical ATR-IR spectra of a single sample at two different pressures, 20 and 50 bar. Only a few relevant peaks can be identified in this figure.

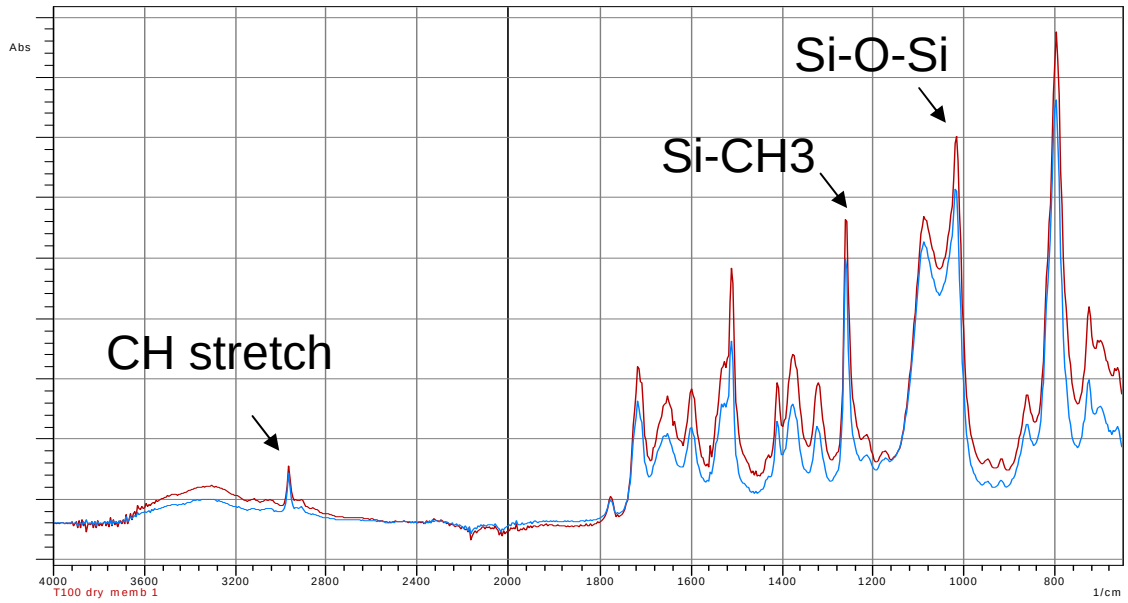

Figure 6.2: ATR-IR spectra of the active layer of the membrane, Solsep 030206, at two different pressures, 20 bar (bottom) and 50 bar (top).

The figure shows an increase in intensity of each peak with the applied pressure. Apart from the increase in absorption, the spectrum remains essentially unchanged. This indicates that no chemical changes have occurred. The overall increase in absorbance is attributed to an increase in sample density. Figure 6.3 shows a particular part of the spectrum (Si-O-Si vibration) for a gradual increase in pressure. As pressure increases, the intensity of the peak also increases.

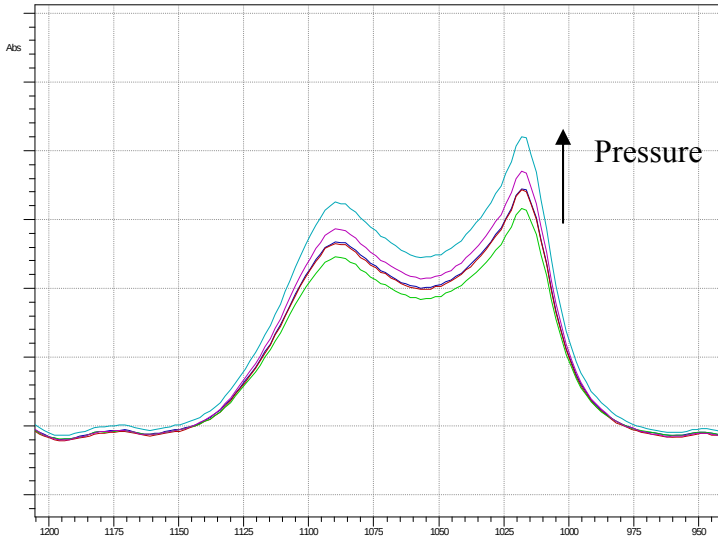

Figure 6.3: Gradual increase of the specific peak Si-O-Si taken of a membrane sample under 10, 20, 30, 40 and 50 bar, respectively.

The total energy absorbed, normalized with respect to the value at 10 bar, is depicted in Figure 6.4 as a function of pressure.

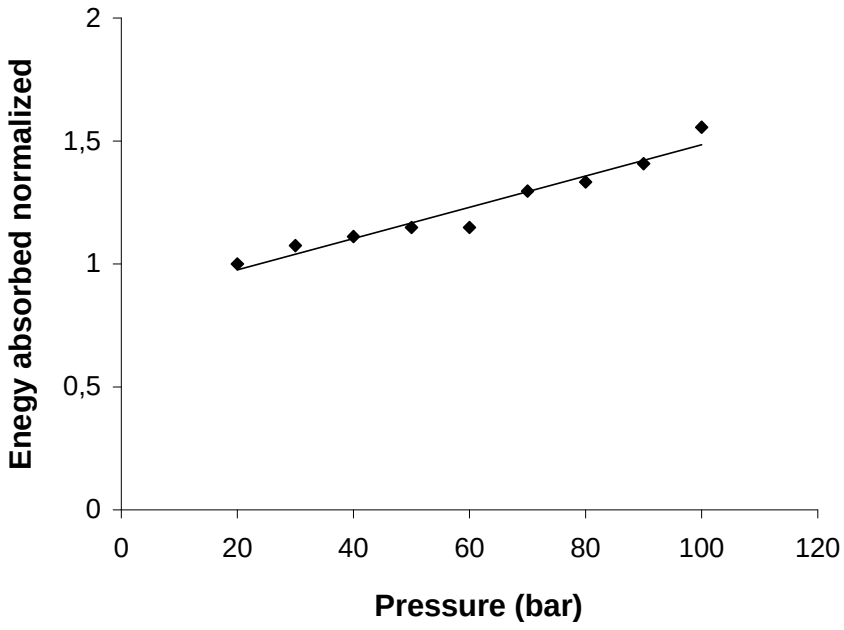

Figure 6.4: Energy absorbed by the active layer of the membrane Solsep 030206 under pressure.

The increase in absorbance, i.e. compaction of the active layer of the membrane, shows an almost linear increase with applied pressure. The linear relation holds even at pressures far exceeding those encountered in most practical applications (max. 50 bar of pressure). The increase in density of the active layer is approximately 5% per 10 bar. Consequently, at the maximum pressures encountered in typical applications the compaction will increase the density of the active layer by approximately 25%.

6.4.1 Reversibility

Figure 6.5 shows data from an experiment in which the pressure has been increased and subsequently decreased in periods of one minute for each pressure. During pressure increase the energy absorbed by the sample increases by 20% at 40 bar. As pressure is reduced the density reaches a final value, which is 13% higher compared to the value before the compaction experiment. This hysteresis indicates that pressure-induced compaction of the active layer is partly irreversible. Hence, membrane performance will be subject to the pressure trajectory applied. The results shown are in a short-term time frame for pressure application. More experiments should be performed in order to understand the reversibility of compaction when a membrane is under pressure for a long period of time of pressure application.

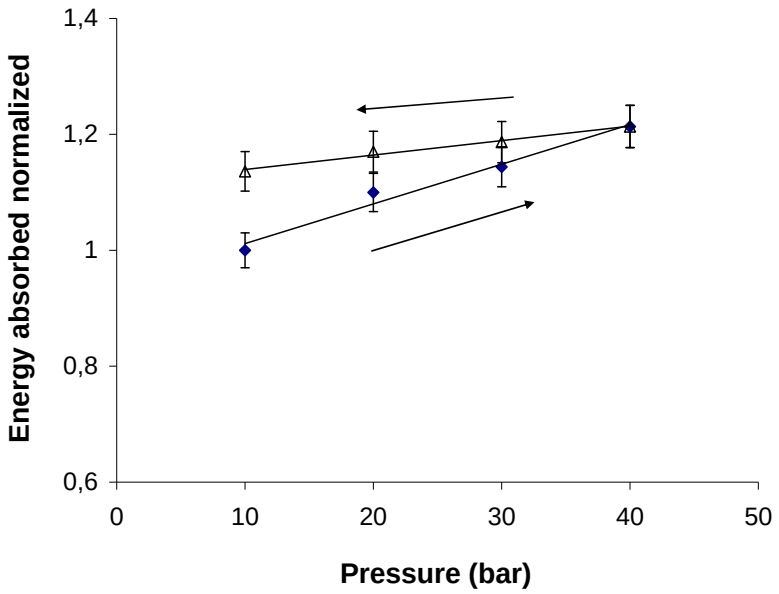

Figure 6.5: Hysteresis pressure experiment - energy absorbed by the active layer of the membrane under pressure.

In Figure 6.6 the change in the overall thickness of the membrane, determined using the micrometer, is depicted for a similar pressure trajectory as compared to Figure 6.5. During the sequential increase in pressure the total thickness of the membrane continuously decreases, reaching 94% of the initial thickness at a maximum pressure of 40 bar. This is equivalent to an average density increase of 6% over the membrane layers. During the subsequent decrease in pressure a further reduction in thickness is observed, reaching 82% of the initial thickness at the final pressure value of 10 bar, equivalent to an increase in density of 18%. The results show that the change in overall density is totally irreversible for the time frame used. The relative values of density increase from the in-situ ATR-IR measurements and the overall density measurements are not in agreement. The results are not surprising considering that the overall measurements include all layers present in the membrane, whereas the ATR-IR approach only reveals changes in the active layer.

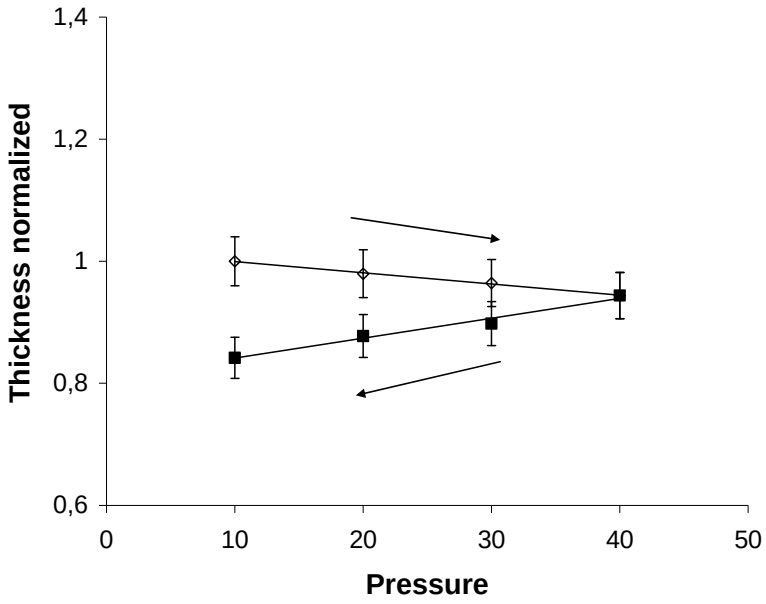

Figure 6.6: Hysteresis pressure experiment – thickness of the membrane taken after pressure has been applied for a period of one minute.

In an actual nanofiltration experiment compaction is accompanied by swelling. Compaction will normally cause an increase in membrane resistance, while swelling is expected to cause a decrease. Results for permeation experiments are depicted in Figure 6.7, for methanol and 1-butanol. For these solvents the extent of swelling will be comparable (see Chapter 5). During the initial increase in transmembrane pressure both solvents show an increase in resistance to transport. This increase is attributed to compaction and is larger for methanol (~80%) as compared to 1-butanol (~15%). For the subsequent reduction in pressure the resistance for transport of methanol shows a continuous increase to twice the initial value. For 1-butanol such a behavior is not observed.

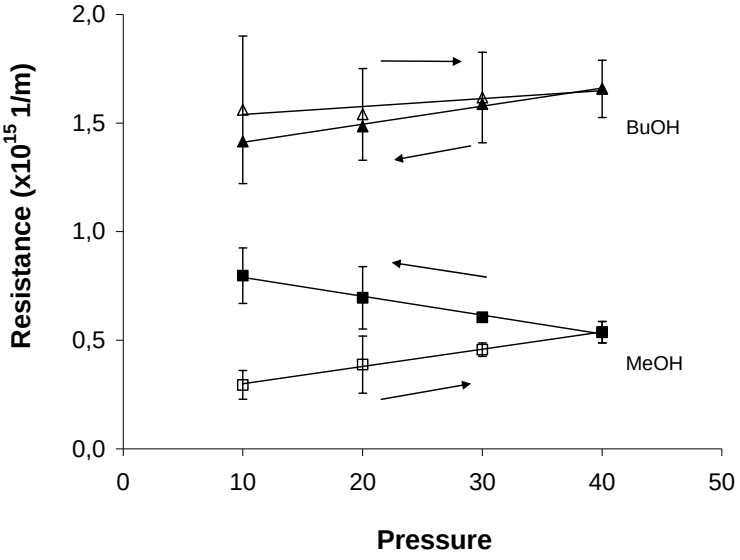

Figure 6.7: Hysteresis permeation experiment using a batch membrane module (see Figure 2.2) for methanol and 1-butanol with the Solsep 030206 membrane.

Compaction shows a direct effect causing a reduction of the flux of methanol but no effect is evident on the flux of 1-butanol. The difference between the two solvents is the dominant transport mechanism (see Chapter 2). The transport of methanol is dominated by viscous transport and takes place in the open spaces of the polymer matrix. The transport of 1-butanol is dominated by diffusive transport and takes place within the crosslinked structure of the polymer. These results show that even for similar molecules, different compaction effects can be expected. The free volume available for diffusive transport in the polymer matrix is not affected in a major way whereas the open space available for viscous transport undergoes a significant change.

6.5 Conclusions

Compaction of the active layer of a commercial membrane has been studied as a function of pressure using ATR-IR. The method here proposed makes a distinction between compaction in the transport determining active layer and the different support layers of the membrane. Results have shown that the two phenomena are not in accordance. For an increase in pressure up to 40

bar the density of the active layer shows an increase of 20%. During subsequent pressure reduction to 10 bar, 7% of the change in density is recovered and an irreversible increase in density of 13% remains. During a similar hysteresis experiment the overall membrane thickness shows a continuous decrease to 80% of the initial value. The change in overall thickness is influenced by all layers present in the membrane and is not directly related to the density change of the active layer.

Permeation experiments show that compaction has a more pronounced influence on transport of methanol as compared to 1-butanol. For 1-butanol transport occurs by diffusion and the membrane resistance is hardly affected by compaction. In contrast, for methanol viscous transport dominates and a continuous increase in resistance is observed during the hysteresis experiment.

References

[1] P. F. Fuls, M. P. Dell, I. A. Pearson, Non-linear flow through compressible membranes and its relation to osmotic pressure, J. Memb. Sci. 66 (1992) 37-43

[2] J. P. Sheth, Y. Qin, K. K. Sirkar, B. C. Baltzis, Nanofiltration-based diafiltration process for solvent exchange in pharmaceutical manufacturing, J. Memb. Sci. 211 (2003) 251-261

[3] D. M. Bohonak, A. L. Zydney, Compaction and permeability effects with virus filtration membranes, J. Memb. Sci. 254 (2005) 71-79

[4] L. Brinkert, N. Abidine, P. Aptel, On the relation between compaction and mechanical properties for ultrafiltration hollow fibers, J. Memb. Sci. 77 (1993) 123-131

[5] K. M. Persson, V. Gekas, G. Tragardh, Study of membrane compaction and its influence on ultrafiltration water permeability, J. Memb. Sci. 100 (1995) 155-162

[6] K. Ebert, D. Fritsch, J. Koll, C. Tjahjawiguna, Influence of inorganic fillers on the compaction behavior of porous polymer based membranes, J. Memb. Sci. 233 (2004) 71-78

[7] R. A. Peterson, A. R. Greenberg, L. J. Bond, W. B. Krantz, Use of ultrasonic TDR for real-time noninvasive measurement of compressive strain during membrane compaction, Desalination 116 (1998) 115-122

[8] V. E. Reinsch, A. R. Greenberg, S. S. Kelley, R. Peterson, L. J. Bond, A new technique for the simultaneous, real-time measurement of membrane compaction and performance during exposure to high-pressure gas, J. Memb. Sci. 171 (2000) 217-228

[9] I. F. J. Vankelecom, K. D. Smet, L. E. M. Gevers, A. Livingston, D. Nair, S. Aerts, S. Kuypers, P. A. Jacobs, Physico-chemical interpretation of the SRNF transport mechanism for solvents through dense silicone membranes, J. Memb. Sci. 231 (2004) 99-108

[10] M. W. Urban, Attenuated total reflectance spectroscopy of polymers: theory and practice, Am. Chem. Soc. (1996), Washington, DC

[11] N. M. B. Flichy, S. G. Kazarian, C. J. Lawrence, B. J. Briscoe, An ATR-IR study of poly (Dimethylsiloxane) under high-pressure carbon dioxide: simultaneous measurement of sorption and swelling, J. Phys. Chem. B 106 (2002) 754-759

[12] T. Guadagno, S. G. Kazarian, High-pressure CO_2-expanded solvents: simultaneous measurement of CO_2 sorption and swelling of liquid polymers with in-situ near-IR spectroscopy, J. Phys. Chem. B 108 (2004) 13995-13999

[13] K. L. A. Chan, N. Elkhider, S. G. Kazarian, Spectroscopic imaging of compacted pharmaceutical tablets, Chem. Eng. Res. Des. 83 (2005) 1303-1310

[14] S. G. Kazarian, K.L. A. Chan, Application of ATR-FTIR spectroscopic imaging to biomedical samples, review article, Biochim. Biophys. Acta 1758 (2006) 858-867

[15] N. Elkhider, K. L. A. Chan, S. G. Kazarian, Effect of moisture and pressure on tablet compaction studied with FTIR spectroscopic imaging, J. Pharm. Sci. 96 (2007) 351-360

Chapter 7

Perspectives

Nanofiltration offers the opportunity to eliminate energy consuming unit operations such as distillation or extraction. However, nanofiltration for the recovery of organic solvents from industrial streams is still in a very early stage of development. In the simplest case nanofiltration involves a solvent, a solute and a membrane. However, for practical industrial applications, multi-component mixtures will be present and chemical and physical phenomena such as sorption, swelling and compaction will have a strong effect on the overall separation performance. The interrelation between these various phenomena is not yet fully understood, preventing adequate prediction of mass transport in solvent nanofiltration. This thesis provides a number of analysis techniques that can be used as tools in strategic development and characterization of thin film polymer membranes. All the presented techniques are aimed at in-situ study of sorption, swelling or compaction in the transport determining layer, both for model systems and commercial membranes in practical applications. They are independent of the solvent environment, time effective and do not require difficult sample preparation or complicated and expensive set-ups. The tools will be beneficial in the development stage, as well as in the industrial application of non-aqueous nanofiltration membranes.

7.1 Membrane development

Traditionally, characterization of sorption, swelling or compaction is directed at the immediate effects of these phenomena on separation performance [1,2]. However, already in a very early stage of membrane development relevant characterization methods can be extremely valuable, for instance for early screening of promising membrane materials [3,4,5]. The work presented in this

thesis marks the opportunities of using characterization techniques to screen membranes and membrane materials on chemical resistance, permeability, sorption, swelling and compaction. The techniques include attenuated total reflectance infrared spectroscopy (ATR-IR), optical interferometry, mechanical thickness measurements and transport studies. The methods proposed are independent of chemical environment, can be further extended to a multi-component approach and can be applied in long and short term experiments. All methods focus on the active layer of asymmetric membranes and hence provide important information on transport determining parameters. Using the characterization tools at an early stage of development will aid a good selection of membranes that can endure prolonged application. In later stages of membrane development, the characterization techniques can aid optimization of membrane material properties for specific applications and conditions.

7.2 Membrane application

The proposed techniques are time effective and relatively simple to implement. As a result, the applicability of the techniques is not limited to membrane development only, but can be further extended to actual industrial applications, for instance for real-time in-situ process monitoring. Characterization of time dependent phenomena such as fouling and concentration polarization in actual applications is very important, because they contribute to a poorer performance and eventual break down of the membrane [6-8]. Here, ATR-IR will be especially beneficial as it enables chemical characterization of fouling layers and can be used to determine sorption and swelling [9]. Recently, flexible fibre optics for mid-infrared ATR-IR analyses have been developed [10]. These infrared probes show high resistance to harsh chemical and pressure conditions and can be included in several strategic places along the membrane module, in contact with the active layer of the membrane. This creates an opportunity to included ATR-IR as an online in-situ control tool. The data acquired will give information on the early changes in the surface chemistry and morphology of the membranes, in particular due to fouling [11] and chemical reactions. This will aid preventing irreversible surface damage as well as the

development of more benign membrane cleaning strategies. Consequently, this will prolong membrane life time.

7.3 The future

As the field of solvent nanofiltration will further develop, the need for characterization methods will increase. The tools presented in this thesis provide only a solution for some of the future questions that will be raised. Further development of the tool box can be done by perfecting the existing collection of tools present both in this thesis and in literature. A logical first step would be to use the existing techniques to simultaneously measure interdependent phenomena. For example, ATR-IR and thickness measurements can be extended to study the simultaneous occurrence of sorption, swelling and compaction. Restrictions here reside mainly on the materials used, in particular for the applications of ATR-IR as a characterization method [12]. In addition, measurements can be directed at multi-component mixtures. For instance, the single experiment retention method can be used to study the implications of using a mixture of solvents on membrane retention. Also potential new characterization techniques for analysis of interdependent phenomena can be envisioned. A particular example is nuclear magnetic resonance that can be used to measure dynamic uptake of solvents in thin polymer layers [13]. This technique can reveal the evolution of a solvent concentration profile inside a thin layer, for instance in combination with a corresponding mechanical response. In addition, new developments in the field of NMR imaging may also enable study of concentration polarisation effects in the boundary layer adjacent to the membrane surface [8].

It should be kept in mind that the application landscape of solvent nanofiltration is very broad and the large progress that can be expected in this field does not allow presenting a complete list of potential future techniques. The value of any new technique will depend heavily on the imminent questions raised by new developments, as well as the applications that will come into scope.

References

[1] K. M. Persson, V. Gekas, G. Tragardh, Study of membrane compaction and its influence on ultrafiltration water permeability, J. Memb. Sci. 100 (1995) 155-162

[2] J. Geens, B. van der Bruggen, C. Vandecasteele, Characterization of the solvent stability of polymeric nanofiltration membranes by measurement of contact angles and swelling, Chem. Eng. Sci. 59 (2004) 1161-1164

[3] P. Vandezande, L. E. M. Gevers, J. S. Paul, I. F. J. Vankelekom, P. A. Jacobs, High throughput screening for rapid development of membranes and membrane processes, J. Memb. Sci. 250 (2005) 305-310

[4] V. Freger, A. Bottino, G. Capannelli, M. Perry, V. Gitis, S. Belfer, Characterization of novel acid-stable NF membranes before and after exposure to acid using ATR-FTIR, TEM and AFM, J. Memb. Sci. 256 (2005) 134-142

[5] C. Wu, T. Xu, M. Gong, W. Yang, Synthesis and characterization of new negatively charged organic–inorganic hybrid materials: Part II. Membrane preparation and characterization, J. Memb. Sci. 247 (2005) 111-118

[6] J. S. Vrouwenvelder, J. A. M. van Paassen, L. P. Wessels, A. F. van Dam, S. M. Bakker, The membrane fouling simulator: A practical tool for fouling prediction and control, J. Memb. Sci. 281 (2006) 316-324

[7] E. R. Cornelissen, J. S. Vrouwenvelder, S. G. J. Heijman, X. D. Viallefont, D. van der Kooij, L. P. Wessels, Periodic air/water cleaning for control of biofouling in spiral wound membrane elements, J. Memb. Sci. 287 (2007) 94-101

[8] J. C. Chen, Q. Li, M. Elimelech, In-situ monitoring techniques for concentration polarization and fouling phenomena in membrane filtration, Adv. Colloid Interface Sci. 107 (2004) 83-108

[9] K. J. Kim, A. G. Fane, M. Nyström, A. Pihlajamaki, Chemical and electrical characterization of virgin and protein-fouled polycarbonate track-etched membranes by FTIR and streaming-potential measurements, J. Memb. Sci. 134 (1997) 199-208

[10] C. B. Minnich, P. Buskens, H. C. Steffens, P. S. Bauerlein, L. N. Butvina, L. Kupper, W. Leitner, M. A. Liauw, L. Greiner, Highly flexible fibre-optic ATR-IR probe for inline reaction monitoring, Org. Process Res. Dev. 11 (2007) 94-97

[11] H. Susanto, S. Franzka, M. Ulbricht, Dextran fouling of polyethersulfone ultrafiltration membranes - causes, extent and consequences, J. Memb. Sci. 296 (2007) 147-155

[12] T. Guadagno, S. G. Kazarian, High-pressure CO_2-expanded solvents: simultaneous measurement of CO_2 sorption and swelling of liquid polymers with in-situ near-IR spectroscopy, J. Phys. Chem. B 108 (2004) 13995-13999

[13] D. Airey, S. Yao, J. Wu, V. Chen, A. G. Fane, J. M. Pope, An investigation of concentration polarization phenomena in membrane filtration of colloidal silica suspensions by NMR micro-imaging, J. Memb. Sci. 145 (1998) 145-158

Acknowledgements

At the end of my master's degree in Lisbon, my objective was to start my career as a chemical engineer by having a traineeship abroad. The last thing on my mind was to spend 4 more years at a university. However I shall never regret the decision to come to Eindhoven. It has been a great experience. For this reason I thank all of you.

Martin for all the long and fruitful discussions. Also for all the support and "gezellige" moments during meetings, dinners and other ETD&C activities. Jos, thank you for all the discussions and opportunities to improve myself in so many aspects. Your vision as professor gives us the freedom to broaden horizons and this creates roads to develop many skills both in a professional and personal level. Gerrald, for all the nice discussions and insight during the project. Your enthusiasm on the subject can only bring positive energy. Petrus for providing us with the membranes for this study and also for the nice discussions. Eero, for the good and always entertaining discussions on infrared spectroscopy. Joost, for all the help during the retention experiments. Your insight on LC-MS was crucial to this work. All the students, Mónica, Ana, Elsa, Joost, Vera, Cátia and Maria for bringing their own special approach and insight. It was great working with all of you. Anton, Chris and Madam for the help building set-ups and solving all kinds of practical problems. Monique for all your valuable work. After so many meetings, talks, coffees, experiments but also sometimes experimental problems, I look back with a smile. It would not have been possible without you and it has been a pleasure to work with you. A special thank you to Nieck for the support and time spent at a crucial time of the project. Leon for all the discussions and chats, good moments spent organizing activities and most important your

friendship. Johan for the “always needed” different point of view and advice. Henny and Zwannet for helping me decipher the Dutch language when I started my life in Eindhoven. All my SPD colleagues for all the nice, fun, insightful, interesting and learning moments during work, coffee breaks, congresses, trips, study tours and other SPD activities. Some of you I will meet again, others I will look back as characters part of a very exciting story. All my friends both here in The Netherlands and in Portugal, although you were not directly involved in this work, thank you for the precious good moments together.

Last but not least the family:

Ao Stefan que me atura todos os dias, mesmo quando eu estou mal disposta ou as coisas não correm como eu quero, e aos pais pelo carinho e atenção. À minha familia que está sempre disponível para uns jantares de fugida quando eu passo por Portugal. É sempre bom matar saudades, eu gosto muito de todos voçês.
Um beijo especial aos meus pais que mesmo estando longe, estão sempre comigo.

Ana

CV

Ana was born on the 30th January 1978 in Abrantes, Portugal. She obtained her Chemical Engineering degree at the Faculdade de Ciências e Technologia/Universidade Nova de Lisboa. After completing a 5 month traineeship on "Water treatment in a submerged membrane bioreactor" in 2002 at Nuon, she applied for a PhD position under the Marie Curie industrial fellowship program. The PhD on "Characterization of polymeric membranes for non-aqueous separations" was started in April 2003 as collaboration between ETD&C B.V. and the Process Development Group at the Eindhoven University of Technology, under the supervision of Dr. Martin Timmer and Prof. Jos Keurentjes. In September 2007 she has started her new job as product developer at Océ-Technologies B.V. in Venlo.